The Extent and Limitations of Correlating Measured Interharmonics and Measured Voltage Fluctuations

by

Brandon L. Eidson

A dissertation submitted to the Graduate Faculty of
Auburn University
in partial fulfillment of the
requirements for the Degree of
Doctor of Philosophy

Auburn, Alabama
December 12, 2015

Keywords: Interharmonics, Voltage Fluctuations, Lamp Flicker

Approved by

Mark Halpin, Professor of Electrical and Computer Engineering
R. Mark Nelms, Chair, Professor of Electrical and Computer Engineering
Stanley J. Reeves, Professor of Electrical and Computer Engineering

Abstract

Amplitude modulation is a well-known cause of voltage fluctuations resulting in luminous lamp flicker. Amplitude modulation can be more generally quantified in terms of interharmonics. The theoretical correlation between interharmonics and lamp flicker has been firmly established analytically. Many have also demonstrated a correlation between measured interharmonics and measured lamp flicker. The feasibility of the attempts to generally correlate the measured values have been explored in this work. This is accomplished by calculating normalized correlation coefficients for measured interharmonics and measured short-term flicker severity for several industrial loads, each for multiple hours. Measurements are made consistent with the International Electrotechnical Commission's standards. It is concluded that measured lamp flicker and measured interharmonics are strongly correlated in general provided particular measured interharmonic phasor pairs are properly combined, weighted and grouped.

Acknowledgments

I want to sincerely thank my committee for understanding and supporting my academic and professional goals. I also want to thank my wife, Claire, for the sacrifices she has made and continues to make to enable me to pursue my (our) various ambitions. And, most fundamentally, *soli Deo gloria*.

Table of Contents

List of Figures

List of Tables

Chapter 1

Introduction

A new method for quantifying and measuring voltage fluctuations is needed. Historically, international standards have focused measurement and emission requirements on the impact of voltage fluctuations on luminous lamp flicker, specifically on the human eye-brain response to luminous output variations of 60 W incandescent lamps. Experience suggested that lamp flicker was the most sensitive effect of voltage fluctuations and that 60 W incandescent lamp performance under conditions of amplitude modulation of the power frequency was a suitable basis for standardization. This led to the development of the IEC flickermeter as described in IEC 61000-4-15 [1].

Although the incandescent lamp and classic lamp flicker will remain an issue in the developing world for some time, the developed world is continually moving away from these lamps. The impact of voltage fluctuations on transformers, motors, non-incandescent luminous lamps, etc may need to be explicitly considered because the magnitudes and frequencies of voltage fluctuations which are considered harmful are different for these devices [2]. Therefore, a more general approach to quantifying and measuring voltage fluctuations is needed. Any new method proposed to serve as the basis for international voltage fluctuation standards would have to meet at least the two following requirements:

1. offer some advantages over the present international standard's approach for representing voltage fluctuation sensitives beyond the incandescent lamp; and

2. produce results consistent with the present international standard's approach (i.e., results consistent with the measurements of the IEC flickermeter of [1]).

One option is to quantify voltage fluctuations in terms of what many call interharmonics, spectral components that are not at integer multiples of the power frequency. This rationale stems from the historic success of basing voltage fluctuations on amplitude modulation and the theoretical equivalence of amplitude modulation and interharmonics. A mathematical expression for a signal with sinusoidal amplitude modulation is shown in (1.0.1).

$$u(t) = U_1 \sin(\omega_1 t)(1 + U_m \sin(\omega_m t + \phi_m)) \tag{1.0.1}$$

U_1 and ω_1 are the magnitude and radian frequency of the power component, and U_m and ω_m are the magnitude and radian frequency of the modulation. The expression in (1.0.1) is equal to the expression in (1.0.2).

$$\begin{aligned} u(t) = U_1 \sin(\omega_1 t) &+ \frac{U_m}{2} \sin((\omega_1 - \omega_m)t - \phi_m) \\ &+ \frac{U_m}{2} \sin((\omega_1 + \omega_m)t + \phi_m) \end{aligned} \tag{1.0.2}$$

It can be seen in (1.0.2) that the amplitude modulation that causes lamp flicker can also be represented as interharmonics. In the case of single-frequency, sinusoidal amplitude modulation, this is expressed as a single interharmonic pair. Because current is not of interest in this dissertation, an interharmonic voltage is referred to simply as an interharmonic.

The existence of international standards for measuring interharmonics increases the potential acceptance of using measured interharmonics for assessing voltage fluctuations [3]. If interharmonics measured in accordance with IEC 61000-4-7 can meet the two previously mentioned requirements, the characterization of voltage fluctuations via interharmonic measurements could be viewed simply as a specific application of a measurement approach already accepted by the technical community.

Furthermore, the results of some prior work indicate that interharmonic measurements meet the previously mentioned requirement of holding promise for advantages over the present IEC standard for measuring voltage fluctuations. Part of the IEC flickermeter is designed in reference to the incandescent lamp flicker perceptibility curve [4]. Similar curves already exist for other types of luminous lamps. Therefore, it is reasonable to suspect that interharmonic measurements could be used to evaluate the flicker severity of other lamps if interharmonic measurements can provide results consistent with the present IEC flickermeter. For example, the authors of [5] and [6] developed an algorithm for estimating lamp flicker severity for both incandescent and fluorescent lamps using measured interharmonics. Interharmonic-flicker curves for several types of lamps are already recorded in [7], and interharmonic limits have been added to IEEE 519-2014 [8] based on lamp flicker due to interharmonics [9]. Also, the analysis in [2] of whether or not an IEC flickermeter could be used to limit low-frequency interharmonic voltages reveals that interharmonic measurements could be used to assess limits for voltage fluctuations, should they exist, in reference to their impact on transformers and AC motors.

Whether or not interharmonic measurements meet the second of the two previously mentioned requirements has not yet been assessed in the literature and will be evaluated in this dissertation. To conclude that interharmonic measurements can produce results consistent with the present standard practice for measuring voltage fluctuations, a general correlation between the measurements must be demonstrated. The following five criteria are desirable in comparing interharmonic measurements and lamp flicker measurements aimed at demonstrating a general correlation:

1. measurements are made consistent with present international standards (primarily [1] and [3]);

2. results are obtained for many hours of field data;

3. results are based on field data from several different loads known for producing voltage fluctuations.

4. recorded results represent gapless, non-overlapping measurement intervals (as required for limit compliance in IEC 61000-4-30 [10]); and

5. comparisons show strong correlation.

A comparison of interharmonic and lamp flicker measurement meeting these criteria does not exist in the literature. Some work has been documented examining the relationship of measured interharmonics and measured lamp flicker [5, 6, 11–13]. However, results are based on too little data from too few industrial loads, and/or measurements are not made in compliance with accepted international standards. These will be reviewed in more detail in Section 3.

The feasibility of correlating lamp flicker measurements with interharmonic measurements is explored in this dissertation. Voltage measurements were made for multiple hours at numerous different industrial loads notorious for causing lamp flicker, such as arc furnaces. Calculations of the interharmonics and lamp flicker severity for the datasets were made consistent with the IEC's measurement standards. The strength of the correlations for each dataset is documented, and a conclusion about the general suitability of correlating interharmonic measurements and lamp flicker severity measurement is drawn. It is concluded that measured lamp flicker and measured interharmonics are strongly correlated in many but not all circumstances, if only interharmonic magnitudes are considered. The two measurements can only be strongly correlated in general if measured interharmonic phasor pairs are properly combined, weighted and grouped.

A review of foundational principles necessary for understanding the issues explored in this dissertation is provided in Chapter 2. An overview of work relating to measuring interharmonics and correlating them to measured lamp flicker is contained

in Chapter 3. The experimental setup and measurement methods are described in Chapter 4. Some correlation results for various types of interharmonic calculations are also given. Chapter 5 contains a detailed mathematical analysis demonstrating the theory behind and providing insight into correlating measured lamp flicker and measured interharmonics. An improved weighted, custom interharmonic grouping method based on the magnitude results of interharmonic pairs combined through phasor addition is developed in this chapter. The experimental results for the improved custom interharmonic group correlated to measured lamp flicker are recorded in Chapter 6. The dissertation concludes in Chapter 7 with implications drawn from the experimental results and suggestions for what research is required next if voltage fluctuation measurement is to be based on interharmonic measurement.

Chapter 2

Review of Relevant Topics

A review of harmonics, the Discrete Fourier Transform and lamp flicker will draw attention to the issues of interest in this dissertation. Much attention is given to the relevant portions of international standards relating to interharmonic and lamp flicker measurement.

2.1 Harmonics and Interharmonics

Several power system concerns fall under the field of power quality. Power system harmonics is one such concern. A harmonic is any voltage or current sinusoidal frequency component in the power system that oscillates at an integer-multiple rate of the fundamental frequency, $f_{H,1}$, or, in other words, any voltage or current with a frequency described by (2.1.1). The harmonic order is denoted as h.

$$f_{H,h} = h \times f_{H,1}, \quad h = 2, 3, 4, ... \tag{2.1.1}$$

Harmonics are produced by nonlinear aspects of the power system. One primary source is power electronic loads (e.g., switch-mode power supplies, motor controllers, etc.).

An interharmonic is any frequency component in the power system that is not an integer multiple of the fundamental frequency component (i.e., any component that cannot be defined as in (2.1.1)) [14]. Interharmonics are most commonly caused by two sources:

1. changes in the magnitude or phase of the fundamental (and/or harmonic) components or

2. power electronic devices that are synchronized to frequencies other than the fundamental [3].

The former group (changes in magnitude or phase of fundamental component) is produced by various types of time-varying loads. Welder machines and laser printers are classic examples of loads that produce sinusoidal or square modulated signals, producing a regular, time-varying load. Loads like arc furnaces produce irregular fluctuating loads. Both produce interharmonics, but arc furnaces and other major industrial loads will be the focus of this dissertation.

Harmonics have various negative effects on the power system. Harmonic currents use additional power that produce no work (I^2R losses). These additional currents decrease the life of equipment by loading them more and by increasing the operating temperature of enclosed equipment (e.g., motors, transformers). Harmonics voltages can also lead to useful life reduction. These problems regularly lead to the installation of overrated equipment, increasing operating costs. Additionally, the power system's large network of impedances regularly contains parallel and series resonant frequency points. If a harmonic current or harmonic voltage has a frequency near a parallel or series resonant point, respectively, either an over-voltage or over-current will occur. For these reasons, power system harmonics are a primary concern of power quality engineers and will continue to be so as the use of more and larger nonlinear components is ever on the rise [15].

Interharmonics cause most of the same problems as harmonics. They cause additional problems because they are causes of over-voltages or over-currents in tuned filters, subsynchronous oscillations, and voltage fluctuations (specifically, lamp flicker).

These problems are exacerbated by the fact that interharmonics cause significant effects even at very low magnitudes. Additionally, their frequencies, amplitudes and peridocities vary greatly, making them very difficult to accurately measure [16].

2.2 The Discrete Fourier Transform and Interharmonics

2.2.1 Theoretical Foundation

Using the Fourier Transform, a continuous, steady-state, periodic function, $y(t)$, can be broken up into a summation of sinusoidal components whose frequencies are integer multiples of the original periodic function. These continuous, infinite-length functions cannot be analyzed using a computer, so the Discrete Fourier Transform (DFT) is used. If $y(t)$ is sampled $p \times N$ times to form the sequence $y[n]$, the form of the DFT is as in (2.2.1).

$$Y[k] = \sum_{n=0}^{pN-1} y[n] e^{-j\frac{2\pi k}{pN}n}, \qquad 0 \leq k \leq pN-1 \tag{2.2.1}$$

The DFT is deduced from the Discrete Fourier Series (DFS). The DFS is a way to analyze discrete, periodic signals (i.e., periodic sequences) and only needs to be calculated across one period (from 0 to pN-1) considering that calculations extended beyond that simply repeat the ones already made. Because of this, the same approach can be taken on discrete, finite signals; the samples are simply treated as one cycle of a periodic, infinite-length signal. So, when viewed this way, the DFT is a frequency analysis of a periodically-extended, finite time-domain signal. If all frequency components present are synchronized with the sampling rate and the number of samples (i.e., the sampling window), the resulting spectral information $Y[k]$ will accurately reflect the spectral content of the originally sampled signal. Otherwise, the spectral leaking phenomenon will occur because the nonsynchronized frequency

components' periodic-extensions will be inaccurate. The waveform perceived by the DFT will be different from the actual waveform.

This same idea can be explained another way. The resolution of the frequency spectrum is determined by the length of the sampled signal $y[n]$. Assume the time-domain signal is sampled at a rate of N times per fundamental cycle (i.e, if the fundamental period is T_1, the sampling period $T_S = T_1/N$). If p is the number of fundamental periods included in the DFT calculation, the frequency resolution $f_{C,1}$ is calculated by (2.2.2) where $f_{H,1}$ is the fundamental frequency of the power system.

$$f_{C,1} = \frac{1}{p(NT_S)} = \frac{f_{H,1}}{p} \tag{2.2.2}$$

Any spectral component that is not an integer multiple of $f_{C,1}$ will not be accurately represented and will bleed into surrounding bins (known as the "picket-fence" effect). If only one cycle is included in the DFT calculation, then only components at integer multiples of the fundamental frequency can be obtained, and, therefore, no interharmonics could be accurately detected. The more cycles used in the DFT, the more resolution is available. For example, consider a function described by (2.2.3)

$$y(t) = 1\sin(2\pi(60)t) + 0.005\sin(2\pi(50)t) + 0.003\sin(2\pi(75)t) \tag{2.2.3}$$

If the DFT time window is 100 ms (six fundamental cycles), only spectral components at integer multiples of 10 Hz can be accurately represented. The 6-cycle DFT results are shown in Figure 2.1. If the DFT time window is changed to 200 ms (twelve fundamental cycles), the frequency resolution is increased to 5 Hz, and both interharmonics are accurately represented (Figure 2.2).

However, increasing the resolution by including more fundamental cycles in the DFT has trade-offs. Firstly, the computational burden is increased, increasing the difficulty of making real-time measurements. More importantly, the DFT also assumes

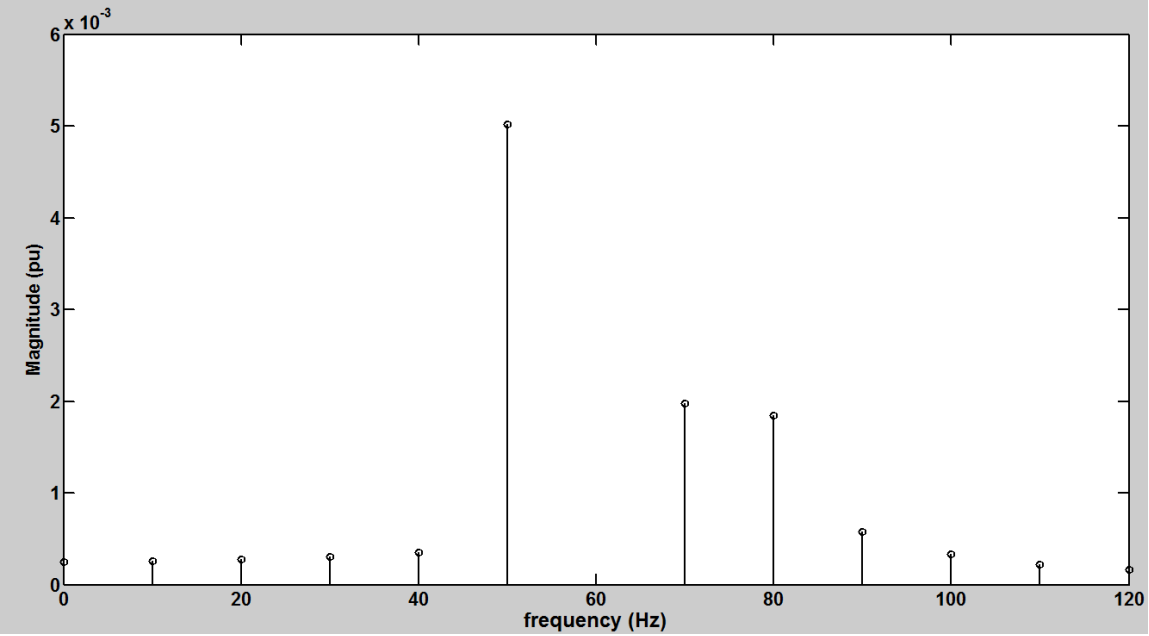

Figure 2.1: Six-cycle DFT of (2.2.3) showing accurate representation of the 50 Hz component and spectral bleeding of the 75 Hz component (the fundamental is not depicted for clarity)

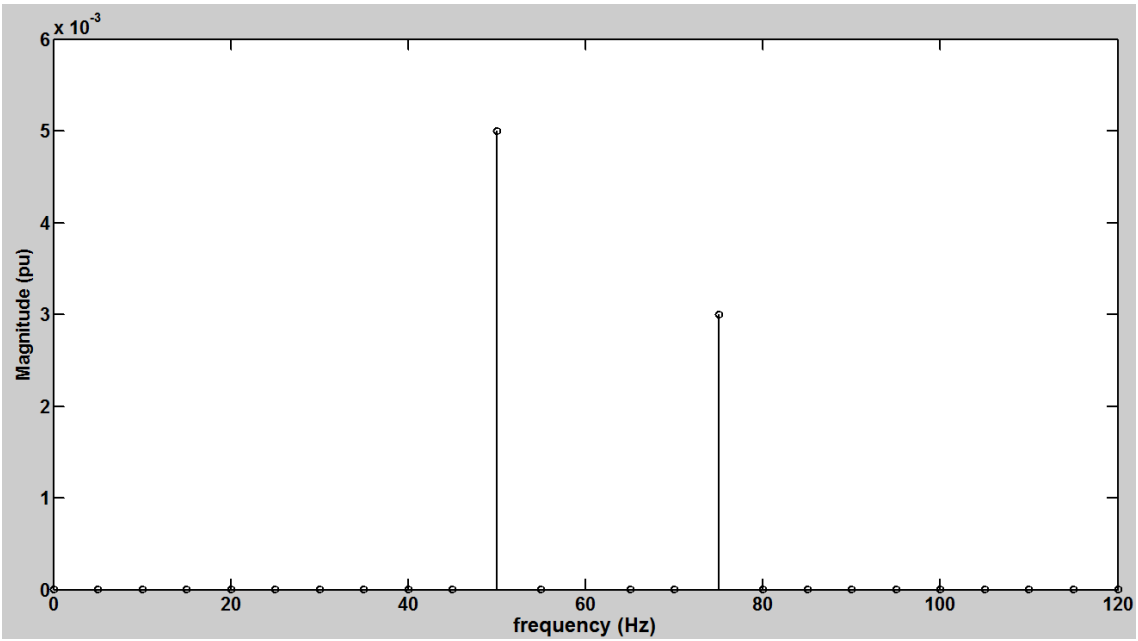

Figure 2.2: Twelve-cycle DFT of (2.2.3) showing accurate representation of the 50 Hz and 75 Hz components (the fundamental is not depicted for clarity)

that the signal is stationary during the time window. If the spectral information present in a signal changes during the observation period, the DFT results will be

inaccurate. In most power system applications, the larger the time window, the more likely the signal will not be stationary. To illustrate, consider a function that, for 150 ms is equal to the function in (2.2.3) but then the magnitude of the 50 Hz component changes to 0.001 (equation (2.2.4)).

$$y_2(t) = \begin{cases} 1\sin(2\pi(60)t) + 0.005\sin(2\pi(50)t) + 0.003\sin(2\pi(75)t), & 0 \leq t < 150ms \\ 1\sin(2\pi(60)t) + 0.001\sin(2\pi(50)t) + 0.003\sin(2\pi(75)t), & 150 \leq t < 200ms \end{cases} \tag{2.2.4}$$

The 12-cycle DFT results are shown in Figure 2.3. Neither the function from $0 - 150$ ms nor $150 - 200$ ms is accurately represented. The trade-off between frequency resolution and stationarity is a fundamental challenge to measuring interharmonics, particularly because their frequencies, amplitudes, and periodicities vary so much.

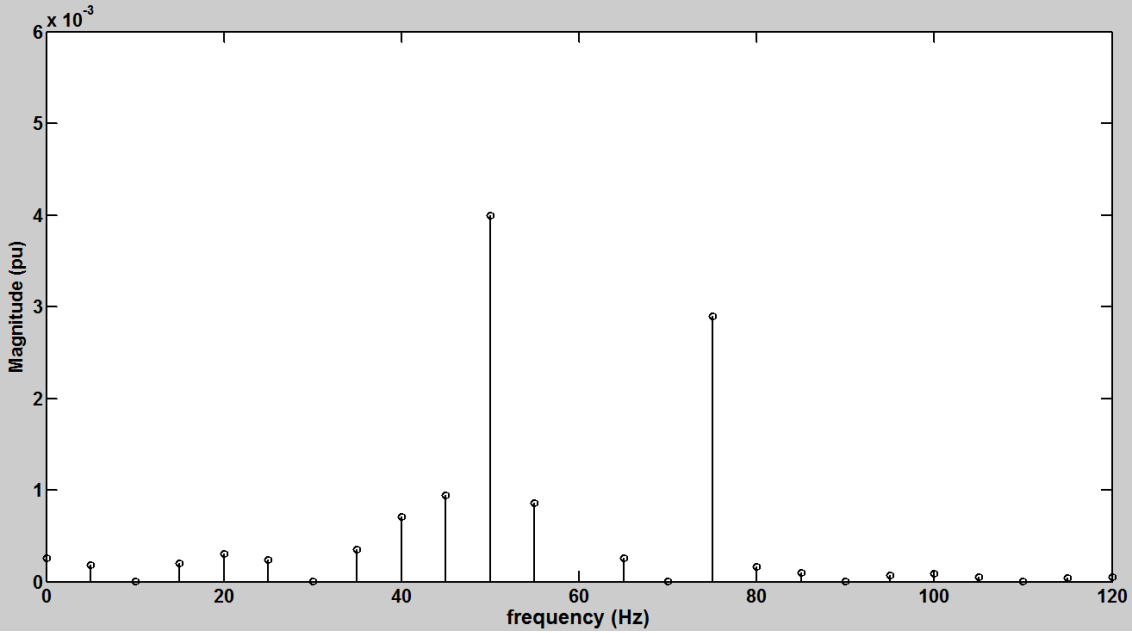

Figure 2.3: Twelve-cycle DFT of a non-stationary signal (the fundamental is not depicted for clarity)

Another fundamental challenge for measuring power system interharmonics related to the first, but worth drawing attention to, is power frequency drift. The frequency of the power component is well controlled, especially in the United States.

However, the fundamental component and, sometimes, harmonics are so much larger than interharmonics that even a slight desynchronization with the fundamental frequency will cause the fundamental component, and maybe harmonics, to make it impossible to accurately detect the presence of nearby interharmonics. Consider again the function in (2.2.3), but the 60 Hz component is changed to 59.99 Hz (see equation (2.2.5)). The 12-cycle DFT results are shown in Figure 2.4.

$$y_3(t) = 1\sin(2\pi(59.99)t) + 0.005\sin(2\pi(50)t) + 0.003\sin(2\pi(75)t) \tag{2.2.5}$$

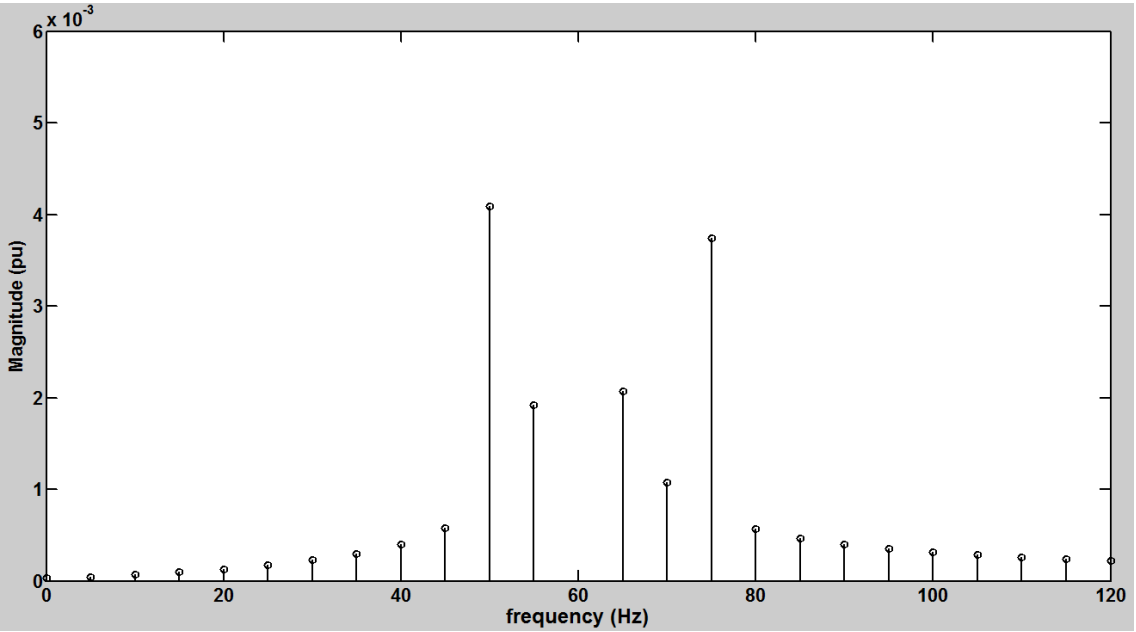

Figure 2.4: Twelve-cycle DFT of the function in (2.2.3) but with the 60 Hz component changed to 59.99 Hz (the fundamental is not depicted for clarity)

Under conditions of fundamental frequency drift, the bleeding from the fundamental component appears as significant interharmonics while small values of interharmonics are needing to be measured due to their potential significant effects. For instance, if a signal described by the function in (2.2.3) persisted for 10 minutes, a flickermeter would measure $P_{st} = 2.225$ ($P_{st} = 1.0$ corresponds to unacceptably large

lamp flicker). Furthermore, measurements made on data to be introduced later in this dissertation recorded interharmonic components each of which had magnitudes 0.2% of the fundamental magnitude or smaller that corresponded to $P_{st} = 2.03$; the faux interharmonics at 55 Hz and 65 Hz caused by the desynchronized DFT of (2.2.5) are about 0.2% of the fundamental (Figure 2.4). The transients caused by arc furnaces are capable of causing significant drifts in the fundamental frequency for the purposes of interharmonic measurement and its relationship to lamp flicker measurement.

2.2.2 Established Measurement Practice

Both IEC and IEEE have developed standards for measuring harmonics: IEC 61000-4-7 [3] and IEEE 519-2014 [8]. IEC 61000-4-7 gives definitions and instructions specifically for measuring interharmonics. A 200 ms time window (12 cycles of the 60 Hz system) is selected, giving the DFT a 5 Hz resolution. $Y_{C,k}$ denotes the RMS value of the spectral component of frequency $f_{C,k} = \frac{k}{p} \times f_{H,1} = k \times f_{C,1}$ and can represent either a voltage value or a current value. Because of the focus on voltage fluctuations in this dissertation, only voltage measurements $U_{C,k}$ will be considered.

Because of the spectral leakage phenomenon, the grouping concept has been introduced in IEC 61000-4-7 in response to the challenge of measuring specific interharmonic components. The h-th interharmonic group is calculated by taking the square root of the sum the squares of all the interharmonic components between the h-th and (h+1)-th harmonics as shown in (2.2.6). The interharmonics included in the first and second IEC interharmonic groups is illustrated in Figure 2.5.

$$Y_{ig,h}^2 = \sum_{k=1}^{p-1} Y_{C,(p\times h)+k}^2 \tag{2.2.6}$$

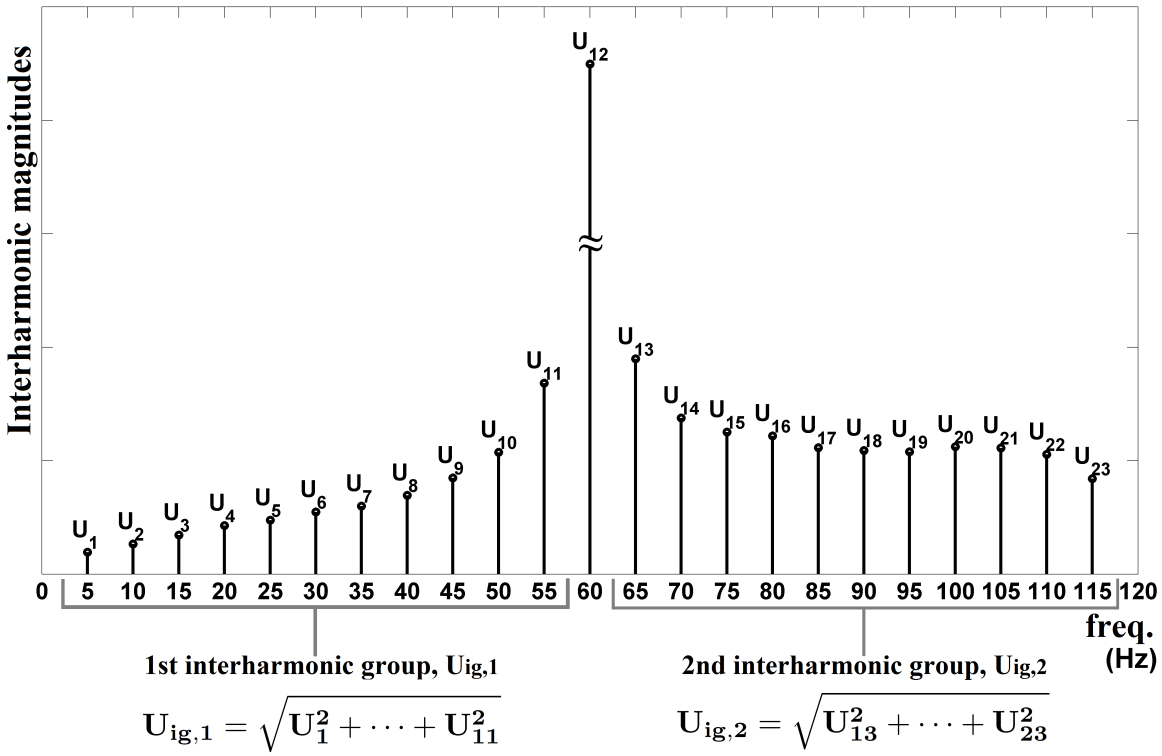

Figure 2.5: Example spectrum showing which interharmonic components are included in the first two interharmonic groups as defined in [3]

The h-th interharmonic subgroup is calculated the same as the h-th interharmonic group, but the interharmonics immediately adjacent to the h-th and (h+1)-th harmonics are excluded (see (2.2.7)).

$$Y_{isg,h}^2 = \sum_{k=2}^{p-2} Y_{C,(p\times h)+k}^2 \tag{2.2.7}$$

Compliance requirements for interharmonic emissions are given in terms of interharmonic groups and subgroups rather than individual interharmonic components. This not only avoids the difficulty of needing to accurately measure individual interharmonic components, but it is also practically justifiable as many problems caused by interharmonics are associated with the effects of their cumulative energies. If an individual interharmonic is not synchronized with the DFT time window, it will

bleed into multiple spectral bins, but the cumulative energies of those bins will coincide closely with the energy of the original interharmonic component [17]. This is based on Parseval's theorem. As a result, the grouping technique can reliably measure the cumulative energy of present interharmonics regardless of whether or not the picket-fence effect occurs.

One exception to the above is if the fundamental component and harmonic components are not synchronized to the DFT time window. In the presence of this fundamental frequency drift, the interharmonic groups' and subgroups' measured energies will include energy really present in the fundamental component and/or harmonic components. Although all harmonics can pose a problem, this is particularly problematic for the fundamental frequency because it can be orders of magnitude larger than the surrounding interharmonics. Therefore, [3] requires interharmonic measurement equipment to include a phase-locked loop (PLL) or other synchronization means so that the time window is fixed to 12 cycles of the [approximately] 60 Hz power frequency. Unfortunately, one negative consequence of interharmonic presence is PLL interference. There are reports in [18] and [19] of digital PLL's fundamental frequency estimates regularly off by $0.01 - 0.02$ Hz; that is sufficient for causing remarkable spectral leakage. Also, the high accuracy required makes analog PLL's less suitable due to hardware variation under different environment conditions. In light of this challenge, an emphasis in this dissertation is placed on a particular strategy for power frequency synchronization.

There is also a recommendation in [3] for smoothing the group calculations using a first-order digital low-pass filter with a 1.5 sectime constant. The equation for this calculation is shown in (2.2.8) where $Y_{oig,h,n}$ represents the interharmonic group measurement filter output of the n-th 200 ms period.

$$Y_{oig,h,n} = \frac{1}{\alpha}(Y_{ig,h} + \beta Y_{oig,h,n-1}) \tag{2.2.8}$$

For a 60 Hz power system using 12-cycle DFT windows, it is recommended that $\alpha = 8.012$ and $\beta = 7.012$.

The IEC requirements for interharmonic measurement relevant to this dissertation are provided in Figure 2.6. Block A and Block B consist of any necessary preprocessing, anti-aliasing filter, fundamental frequency synchronization scheme and sampler. These are combined and thought of as one block in this dissertation because of the particular scheme implemented for fundamental frequency synchronization. Block C represents the calculation of the 12-cycle DFT as shown in (2.2.1). The output of Block C are the spectral components $U_{C,k}$. Block D calculates the interharmonic groups $U_{ig,k}$ and subgroups $U_{isg,k}$. In the attempt to correlate interharmonic voltage measurements with voltage flicker, a custom grouping method is attempted that is not directly outlined in [3] or [8] but is suggested by how a standard flickermeter works. Block D will also represent this custom grouping method calculation, and its output will be noted as U_{cig}. Because there is only one custom interharmonic group, no index k is needed in the subscript. Block E is the smoothing filter.

2.3 Voltage Fluctuations and The Flickermeter

Another major area of power system quality is voltage fluctuations. Voltage fluctuations can cause problems for power system components such as transformers, motors, and generators [20]. However, international standards have historically focused measurement and emission requirements on the impact of voltage fluctuations on luminous lamp flicker, specifically on the human eye-brain response to luminous output variations of 60 W incandescent lamps. Experience suggested that lamp flicker was the most sensitive effect of voltage fluctuations and that 60 W incandescent lamp performance under conditions of amplitude modulation of the power frequency was a suitable basis for standardization. This led to the development of the IEC flickermeter as described in IEC 61000-4-15 [1]. Amplitude modulation of the voltage at the

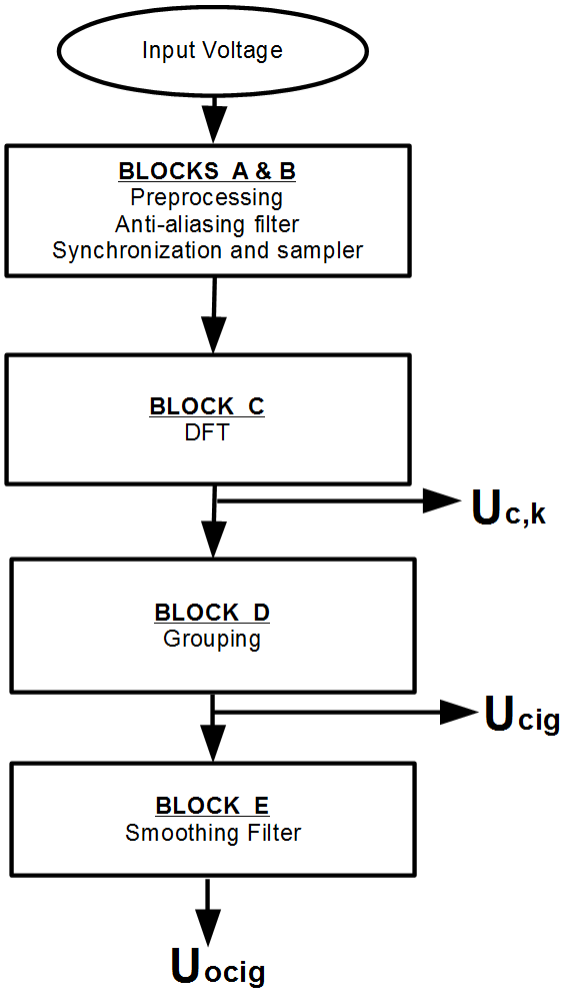

Figure 2.6: Block diagram summary of harmonic measurement instrument requirements according to IEC 61000-4-7.

fundamental frequency can also be described in terms of power system interharmonics as shown in (1.0.2).

How to build a device to measure flicker severity for any type of voltage fluctuation is described in [1]. This standard is followed in this dissertation, treating the short-term flicker severity P_{st} as the measure of voltage fluctuation. The instrument is described in five sections or blocks, which are illustrated in Figure 2.7. Block 1 describes the input voltage adapter which normalizes the input and allows the flicker

level to be determined independent of the actual voltage level. Block 2 is the squaring multiplier that simulates a filament lamp's behavior. The first half of Block 3 (Block 3a) uses a sixth-order, low-pass butterworth filter and a first-order, high-pass filter to remove any dc content and the doubled main frequency content from Block 2; the cut-off frequencies are 0.05 Hz and 42 Hz, respectively. The second half of Block 3 (Block 3b) uses a weighting filter to simulate the human visual system. The highest weight is on 8.8 Hz, meaning an interharmonic at 50 Hz or 70 Hz should have the highest impact on lamp flicker measurement. Block 4 is composed of a squaring multiplier and a first-order, low-pass filter with an RC time constant of 300 ms, and the output is defined as the instantaneous flicker sensation P_{inst}. Block 5 is an online statistical analysis that determines the short-term flicker severity P_{st}, usually a 10 minute value. An output value of $P_{st} = 1.0$ corresponds to an unacceptable amount of customer complaints about lamp flicker [9].

In some instances, it may be necessary to calculate the flicker severity over a period of time that is longer than what the P_{st} result provides. Thus, a long-term flicker severity assessment is calculated using (2.3.1) and some determined number (usually 12) of the previous P_{st} results. The P_{st} measurement will be focused on in this dissertation.

$$P_{lt} = \sqrt{\frac{\sum_{i=1}^{N} P_{st,i}^3}{N}} \tag{2.3.1}$$

2.4 Standardized Measurement Techniques for Power Quality

Techniques for making various power quality measurements for compliance evaluation (Class A devices) are standardized in [10]. This standard requires gapless, non-overlapping measurements of short-term flicker severity and interharmonics. Measurement aggregations over 3-second and 10-minute time intervals are also required for interharmonics. Various assumptions in the interharmonic measurement process,

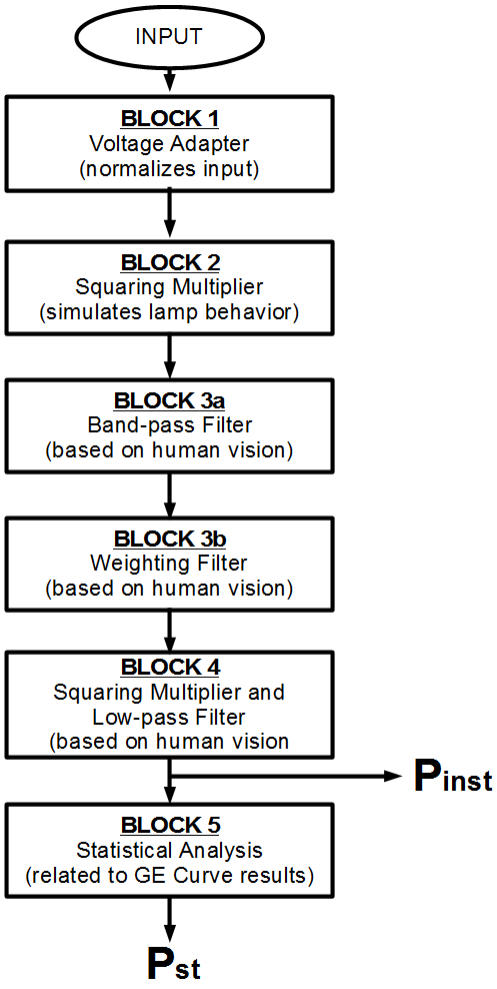

Figure 2.7: Functional block diagram of flickermeter according to IEC 61000-4-15

such as stationarity, will often be incorrect, so a longer observation period often provides more usable result. Because each interharmonic measurement, according to [3], is made over an approximately 200-ms period, approximately 3000 interharmonic measurements are aggregated for the 10 minute measurement (10 min. = 600 sec. = 3000 $\times$ 200 ms). This aggregation is performed as shown in (2.4.1) where $U_{k,n}$ represents the n-th 200 ms measurement of the RMS voltage of the $(k \times 5)$-Hz interharmonic component. Because this is an accumulation of energies, an RMS value is

calculated (i.e., a geometric average is calculated).

$$U_{k,10min} = \sqrt{\frac{\sum_{n=1}^{3000} U_{k,n}^2}{3000}} \tag{2.4.1}$$

This same aggregation can be made for an interharmonic group. The 10-minute interval will be used for aggregating interharmonics and interharmonic groups in this dissertation in order to directly compare them with short-term flicker severity measurements and remain in compliance with established international practices.

Chapter 3

Literature Review

Interharmonics and their relationship to lamp flicker have been of interest to the academic community for the past couple decades. The following is an overview of literature pertaining to interharmonic measurement, particularly under conditions of power frequency drift, and the relationship of interharmonic and lamp flicker measurement.

3.1 Interharmonic Measurements

There exists a great deal of work attempting to mitigate one or more of the challenges of measuring interharmonics.

Most innovative methods for interharmonic detection and measurement are based on using Prony's method or non-rectangular windows in the DFT. Although Prony-based methods are capable of very high precision [22], they are inherently computationally intensive compared to DFT-based methods and highly sensitive to noise in actual measured signals. Furthermore, very few applications require precise measurement of individual interharmonic components; group measurements are typically sufficient.

Increasing the IEC 61000-4-7 sample window to include enough cycles to create a 1 Hz frequency resolution ($f_{C,1} = 1$ Hz) is proposed in [23]. For a 60 Hz system, a 60-cycle DFT window would be required. No explanation is provided as to why the benefit of this increased resolution outweighs the increased likelihood of performing the DFT on a non-stationary signal. The algorithm is only demonstrated using a

generated test signal with an interharmonic component at 53 Hz, illustrating that the 1 Hz DFT results can accurately represent it while the 5 Hz DFT results (consistent with [3]) cannot. It is not clear that there would be benefits for measuring interharmonics by increasing the observation window when measuring the voltage signal at, for example, an arc furnace.

3.2 Dealing with Fundamental Frequency Drift

The challenge of measuring interharmonics during conditions of power frequency drift is addressed by several works. Given that, theoretically, under perfect amplitude modulation, interharmonic pairs around the power frequency should be symmetrical ($U_{C,h-k} = U_{C,h+k}$ if h equals the spectral number of the power frequency), an iterative search for the fundamental frequency based on which interharmonic component of the pair is larger is proposed in [24]. A selection of "how far" from the fundamental frequency to group spectral powers must be made, and the appropriate group bandwidth will vary depending on the situation. This method would not work, however, if perfect amplitude modulation did not exist—frequently the case with irregularly time-varying loads. Furthermore, the demonstration of the iterative method working with real or even realistic data was lacking. In particular, actual interharmonics are typically orders of magnitude smaller than the fundamental while [24]'s only numerical example had interharmonic magnitudes from 7% - 30% of the fundamental.

The algorithm in [13] attempts to improve accuracy of interharmonic measurements in the presence of fundamental frequency drift by vector subtracting out an estimate of the interharmonic bleed from the fundamental. This is accomplished by finding the DFT results of the original signal and subtracting out DFT results from a synthesized signal containing only the fundamental component—using the magnitude of the fundamental frequency from the original DFT and an estimate of the fundamental frequency from zero crossings. Although the simulated results were strong,

one drawback of this approach is that it cannot account for the error present in the DFT calculation of the original signal's fundamental component magnitude (if there is bleeding, the calculated fundamental magnitude will always be smaller than the actual magnitude). The synthesized signal used to determine what the interharmonic bleed will be is constructed using a fundamental component containing, if bleeding has occurred, inherent error. Verification of the algorithm is attempted using experimental data from two AC arc furnaces, but only portions of the results are displayed (five, one minute intervals from each arc furnace) without explanation as to why these portions were chosen over others. It is not clear whether or not the results would be reliable in general.

A very similar approach is taken in [25], except the fundamental frequency is determined using the odd points interpolation correction method, the subtracting-out of the reconstructed signal is performed in the time domain and the algorithm continues this process starting with the largest interharmonic. This approach has an advantage over [13] in that only one DFT is performed, but continuing to iterate through interharmonics is unnecessary for actual power system applications because the bleeding of interharmonics is trivial compared to the fundamental component and few applications need information beyond what the IEC 61000-4-7's grouping methods will supply. The algorithm in [25] is only tested using simulated data.

The work in [17] explores the effects of using a Hanning window rather than a rectangular window when calculating the DFT to mitigate the effects of spectral leakage, primarily due to fundamental frequency deviations. IEC 61000-4-7 allows such an approach in cases of loss of synchronization, although the measurement results may not be used for determining compliance [3]. Nonetheless, the analytical and experimental results show better interharmonic measurement resilience under spectral leakage using a Hanning window rather than a rectangular window, especially when the DFT time window is doubled in length. However, the improvements were far

more moderate when considering frequencies near the fundamental—the components relevant to lamp flicker. Also, the need to experimentally calculate the gain to compensate for the Hanning window's larger main lobe width is a drawback to applying this method in general.

The approaches in [13] and [25] are very similar to an approach previously proposed in [26] which builds on the work in [17]. After the DFT is taken, a frequency domain interpolation is performed to more accurately estimate the fundamental and harmonic components. These components are filtered out of the original measured signal in the time domain, though they mention this could occur in the frequency domain. Another DFT is calculated for this filtered signal, and the interharmonics are then evaluated. This approach improves over the previously described methods because the frequency domain interpolation will undo some of the inaccurate measurement of the fundamental magnitude due to leakage. The need for using a Hanning-based "opportune window" remains, raising questions as to whether or not the frequency interpolation could be reliably used in general.

The same authors of [17] and [26] propose another method for mitigating spectral leakage in the presence of fundamental frequency drift in [27]. Synchronization to the fundamental is attempted by first estimating the actual fundamental period. The actual fundamental period is estimated by searching for the number of samples to include in the DFT that maximizes the magnitude of the fundamental spectral component. When the magnitude of the fundamental component is maximized, synchronization is maximized. Analytical and experimental results suggest that the synchronization is very sensitive to estimation uncertainty, and results only seemed reliable when the instantaneous estimated values for the fundamental period were averaged over 200 ms and used with a Hanning window. The experimental tests utilized a sampling frequency of 25 kHz. The concept of estimating the actual fundamental

period will be used in this dissertation to accomplish synchronization, but the fundamental frequency estimation and synchronization will be accomplished differently, requiring less computation and being more generally applicable.

3.3 Correlating Measurements of Interharmonics and Lamp Flicker

The relationship of interharmonics and lamp flicker (and/or, more broadly, voltage fluctuations) has also been the attention of much study. A thorough evaluation as to whether or not low-frequency interharmonic limits can be based on flickermeter measurements is found in [2]. The conclusion based on the analytic and numerical results is that the interharmonics could be present at extremely harmful levels (from the perspective of ac motors, transformers and/or turbogenerators) while the flickermeter is recording low levels of short-term flicker severity. This should be expected because flickermeters are most sensitive to frequencies that do not necessarily correspond to problematic frequencies for other electrical equipment. Therefore, for general compliance purposes, the flickermeter cannot substitute for the spectral analysis as outlined in [3], even specifically for low frequencies.

Nonetheless, interharmonic voltage limits focused exclusively on flicker severity have been proposed in [9] via a theoretical analysis of a standard flickermeter's response to a single interharmonic in one of the following frequency ranges: less than 18 Hz, 19-21 Hz, or greater than 21 Hz. It was determined that the IEC flickermeter may need to have changes made to the types of filters it utilizes if it is to be used to assess interharmonic limits. The work in [7] suggests interharmonic limits based on RMS fluctuation and peak fluctuation, the latter aimed at limiting interharmonics based on fluorescent lamp flicker—which an IEC standard flickermeter is not designed to measure. Even more interharmonic-flicker curves for various types of lamps are recorded in [21].

Reasonable correlation between measured lamp flicker and measured interharmonics is claimed in [11]. Interharmonic groups (as defined in [3] and described in this dissertation by (2.2.6)) are measured simultaneously with lamp flicker; both are calculated over 10-minute and 2.5-hour intervals for several days at one location. The measurement results are plotted over time: one plot for the interharmonic group between the first and second harmonic and the interharmonic group between the second and third harmonic and one plot for P_{st}. There appears to be good correlation between the plots, but there is no further quantification of the correlations. No custom interharmonic group tailored to the flickermeter was utilized.

A few papers record attempts to estimate flickermeter output based on measured interharmonics. Analytical models of the flickermeter's response to a voltage with sinusoidal amplitude modulation and a voltage with a superimposed interharmonic tone are developed in [5] and [6]. Once the spectral components of interest are determined, the components are weighted in inverse proportion to the flicker perceptibility curve. The analysis aims to include all spectral components corresponding to the amplitude modulation that a flickermeter responds to and the spectral component to which, in the judgment of [5]'s authors, the flickermeter ought to respond. This judgment is made based on the fact that the flickermeter is designed specifically to measure spectral components that cause incandescent lamp flicker, while other spectral components cause lamp flicker in various types of fluorescent lamps. Numerical tests showed the method could reasonably predict flicker output. Both the numerical and lab tests suggest that, if lamp flicker measurement is to be extended beyond incandescent lamps, a method based directly on interharmonic measurement may be more suitable than the current IEC flickermeter implementation. There is much merit in this method because of its strong theoretical foundation. The focus in these papers, however, is not specifically on correlating interharmonic measurements to measurements made by a standard IEC flickermeter but on using interharmonics

to make measurements that a flickermeter "ought" to make. Also, reference is made in [6] to the need to account for the effects of phase angles of the interharmonic components to account for how they combine to affect lamp flicker measurement, but these combinations are accomplished simply through adding the amplitudes of interharmonics to consider only the worst-case scenario. Making worst-case estimates of lamp flicker based on interharmonic measurements accomplishes something different than evaluating whether or not interharmonic measurements can be correlated to standard lamp flicker measurement.

Similarly to [5] and [6], the mathematical relationship between instantaneous flicker sensation and interharmonic voltages is derived in [12] so that short-term flicker severity estimates can be made from interharmonic measurements. The analytic expressions were validated using voltage measurements from a DC arc furnace and an AC arc furnace. The short-term flicker severity estimates differed very little from the flickermeter measurements for the time intervals shown, but the paper does not give explanation as to why these time intervals were selected out of all the measurements available. This paper does not record whether or not most time intervals' percent error were as low as the ones recorded. Half the results were made by deviating from the IEC 61000-4-7 standard DFT time window.

The work in [13] extends its approach for interharmonic measurement in the presence of fundamental frequency drift to lamp flicker evaluation. The interharmonic measurements are weighted and grouped based on the IEC flickermeter requirements. There are strong correlations between their method's estimations and the flickermeter's calculations when simulated voltage waveforms are used. Some of the experimental results, based on AC arc furnace data, are also strong, but, once again, very few results are displayed, and the displayed results are based on an unjustified selection of time intervals.

Listed in this review are several algorithms for measuring interharmonics and some methods for estimating lamp flicker measurement based on interharmonic measurement. Most of the works have focused on the theoretical relationship between interharmonics and lamp flicker. The results of some of the literature suggest that interharmonic measurement and lamp flicker measurement are strongly correlated and hold promise that lamp flicker measurements could be reasonably estimated based on interharmonic measurements. However, the literature does not provide sufficient information to conclude that these correlations exist in general. Results are based on too little data from too few industrial loads, and/or measurements are not made in compliance with accepted international standards, particularly [10]. More experimental results from more loads are needed if one is to say whether or not a strong correlation exists in general.

Chapter 4

Experiment Implementation and Initial Approaches to Correlating Measurements

What follows is a record of how the experiments used in this dissertation were implemented and how correlation is quantified. Various interharmonic values and groups were measured and calculated and correlated to measured lamp flicker. An overview of what data is on hand and how calculations were performed is first provided.

4.1 Experiment Implementation

A-phase voltage measurements have been made at six industrial loads prone to producing lamp flicker. These will be referred to as Dataset 1 through Dataset 6. Dataset 2 is of particular interest because it refers to a facility with the lamp flicker mitigation equipment installed. A summary of information relating to the measurements is found in Table 4.1.

Dataset #	**Sampling rate (Hz)**	**Measurement time (hours)**
1	1920.123	16.3
2	1920.123	5.8
3	5000	3.5
4	5000	3
5	5000	2.5
6	5000	2.3

Table 4.1: Summary of experimental data

A software implementation of the flickermeter has been developed using MATLAB based on the specifications of IEC 61000-4-15 outlined in Section 2.3. It was verified using the standard's specified test points. The first minute of data was read in and processed but not included in the results in order that the filters' initial transients could pass. Thereafter, the short-term flicker severity P_{st} was calculated and saved every 10 minutes. MATLAB was also employed to perform the interharmonic calculations described in Section 2.2 and the various interharmonic groups still to be described. The voltage samples were first passed through a fifteenth-order low-pass Butterworth filter with 150 Hz cut-off frequency to remove spectral content not of interest in this dissertation.

To assess correlation, normalized correlation coefficients were calculated for various interharmonic measurements versus lamp flicker measurement. The normalized correlation coefficient is the measure of linear relationship between two variables, where R = 1 is total positive correlation, R = −1 is total negative correlation and R = 0 is no correlation [28]. For linear fits, R is the square-root of R^2, the coefficient of determination. Normalized correlation coefficients were calculated by normalizing the covariance of the interharmonic aggregation averages and the P_{st} values $C(U_k, P_{st})$ as in (4.1.1). The covariance was calculated by (4.1.2) where A is the number of 10 minute values, $U_{k,10min,x}$ is the x-th 10-minute average of the k-th interharmonic component, and $\langle U_k \rangle$ and $\langle P_{st} \rangle$ is the mean of all the 10-minute values of the k-th interharmonic component and P_{st} measurements, respectively. A normalized correlation coefficient of 1.0 corresponds to perfect positive correlation.

$$U_{C,k} vs. P_{st} = \frac{C(U_k, P_{st})}{\sqrt{C(U_k, U_k) C(P_{st}, P_{st})}} \tag{4.1.1}$$

$$C(U_k, P_{st}) = \frac{\sum_{x=1}^{A} (U_{k,10min,x} - \langle U_k \rangle)(P_{st,x} - \langle P_{st} \rangle)}{A - 1} \tag{4.1.2}$$

In order to help visualize the correlation, scatter plots for datasets especially of interest were also generated relating the P_{st} values to the corresponding 10-minute interharmonic values. A linear best fit line (a first-order, least-squares error minimization) was added to the plots.

The first calculated correlation coefficients were between the individual 10-minute interharmonic component measurements and corresponding short-term flicker severity measurement, U_k *vs.* P_{st}. These values are notated as R_k. These correlation coefficients were first calculated using interharmonics that were measured without a technique for synchronizing the time samples to the fundamental frequency component. The resulting correlations $\mathrm{R}_{k,NoSync}$ for the first two datasets are shown in Table 4.2. For quicker interpretation, the subscripts of the interharmonic components have been labeled with their frequency value; e.g., R_{11} has been changed to R_{55Hz}.

These correlation results were worse than expected. It was also found that these 10-minute aggregations of the interharmonic components' magnitudes were exponentially increasing in size as the frequency approached the fundamental (an example stem plot for Dataset 2 is shown in Figure 4.1). This suggested that the fundamental component was bleeding into the other bins, and, therefore, that the fundamental frequency was drifting sufficiently from 60 Hz such that a scheme for synchronizing time samples to the fundamental frequency had to be considered.

A synchronization technique similar to [27] was implemented for the interharmonic measurements. Rather than measuring 200 ms of data using some kind of phase-locked loop, 25 zero-crossings were detected (corresponding to 12 cycles). The exact time window corresponding to exactly 12 cycles, T_{window}, was estimated using the sampling frequency and linearly-interpolating the times of the first and last zero-crossing. See (4.1.3) and Figure 4.2.

$$T_{window} = t_1 + (n-3)T_s + t_{25} \tag{4.1.3}$$

Interharmonic Component 10 min. Avg.	**Dataset 1 Correlation**	**Dataset 2 Correlation**
$R_{5Hz,NoSync}$	0.1640	0.3556
$R_{10Hz,NoSync}$	0.2180	0.3658
$R_{15Hz,NoSync}$	0.2815	0.3748
$R_{20Hz,NoSync}$	0.3152	0.3821
$R_{25Hz,NoSync}$	0.3377	0.3887
$R_{30Hz,NoSync}$	0.3594	0.3874
$R_{35Hz,NoSync}$	0.3684	0.3881
$R_{40Hz,NoSync}$	0.3742	0.3815
$R_{45Hz,NoSync}$	0.3643	0.3704
$R_{50Hz,NoSync}$	0.3393	0.3530
$R_{55Hz,NoSync}$	0.2904	0.3370
$R_{65Hz,NoSync}$	0.3209	0.3427
$R_{70Hz,NoSync}$	0.4240	0.3747
$R_{75Hz,NoSync}$	0.5117	0.4128
$R_{80Hz,NoSync}$	0.5812	0.4453
$R_{85Hz,NoSync}$	0.6362	0.4728
$R_{90Hz,NoSync}$	0.6812	0.4939
$R_{95Hz,NoSync}$	0.7255	0.5102
$R_{100Hz,NoSync}$	0.7684	0.5260
$R_{105Hz,NoSync}$	0.8135	0.5636
$R_{110Hz,NoSync}$	0.8639	0.6394
$R_{115Hz,NoSync}$	0.8609	0.6302

Table 4.2: Correlation coefficients relating individual interharmonic component 10 minute values with corresponding P_{st} values where time samples were not first synchronized to the fundamental frequency before interharmonic measurements

This approach differs from [27] by how the fundamental frequency is estimated. No search method is utilized, and the 200 ms average is already inherent. All the samples are then resampled to the exact 12 cycle window before calculating the DFT. This ensures the fundamental frequency exists at some integer number of $f_{C,1}$, which

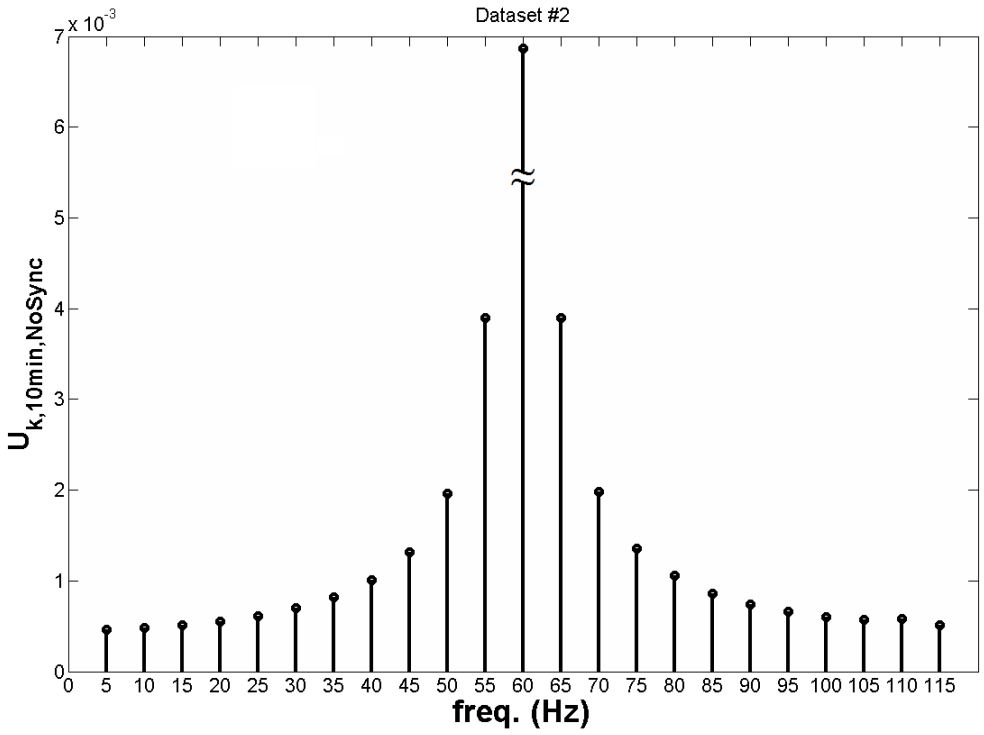

Figure 4.1: Magnitudes of individual interharmonic components's 10 minute aggregation when time samples are not synchronized to the fundamental frequency.

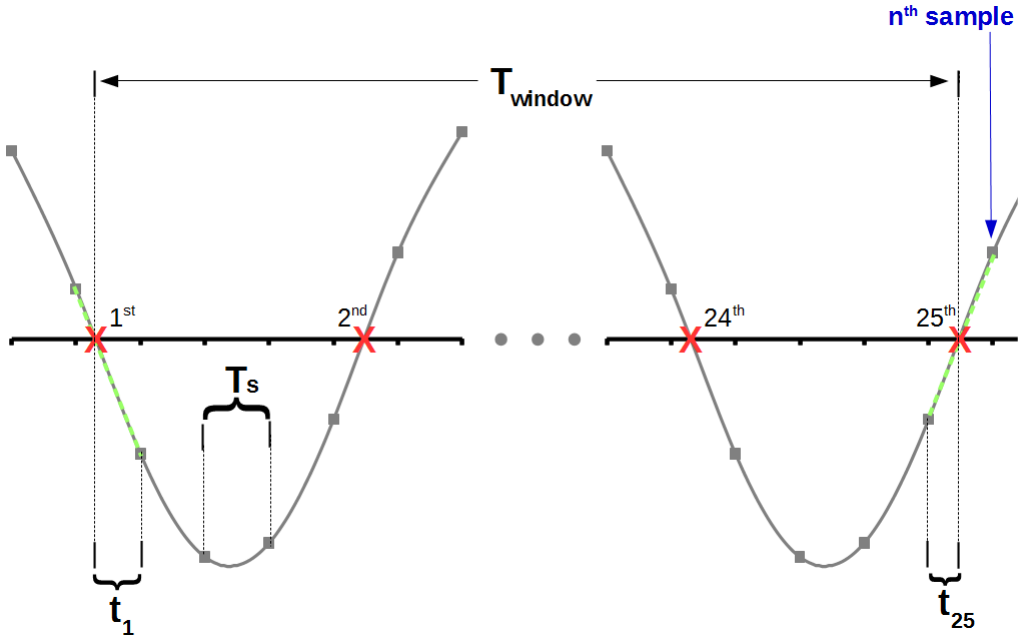

Figure 4.2: Graphical depiction of variables used to estimate time window corresponding to exactly 12 fundamental cycles

will not equal exactly 5 Hz if the DFT time window is not exactly 200 ms, and, therefore, spectral leakage due to fundamental frequency drift is allayed. All datasets were resampled to 32 samples per cycle (1920 Hz), regardless of the original sampling rate. After resampling, another fifteenth-order, low-pass Butterworth filter with a 150-Hz cutoff frequency was used to eliminate the spectral content created from linearly interpolating samples. An overview of this synchronization technique is depicted in Figure 4.3.

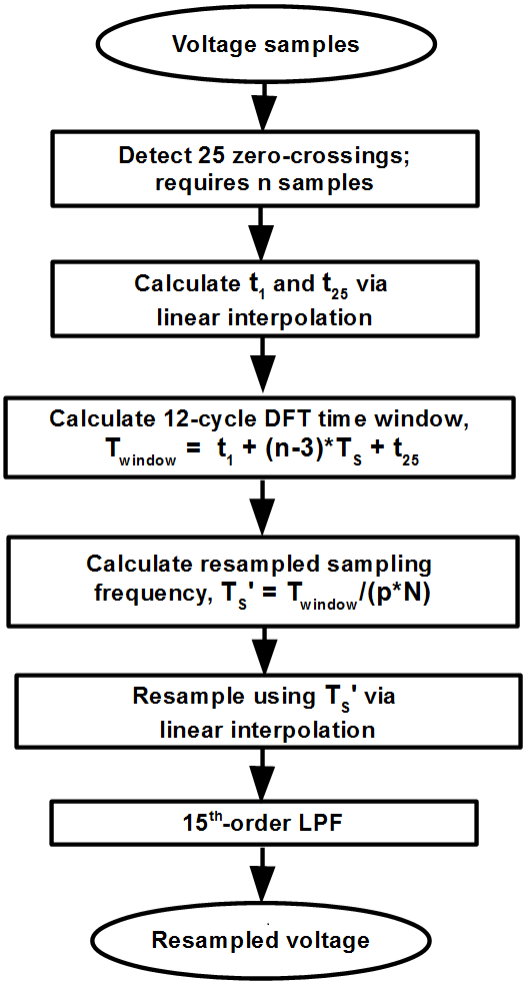

Figure 4.3: Overview of synchronization method used to mitigate spectral leakage due to fundamental frequency drift

Interharmonic components' 10-minute aggregations were approximately 400% to 500% smaller when using the synchronization technique as opposed to when no

synchronization scheme was utilized. This is explained by a large portion of the fundamental component bleed being removed from the interharmonic bins when using the synchronization technique. Although the exact correlation results will be given in the next section, Figure 4.4 shows a scatter plot of all Dataset 2's short-term flicker severity measurements versus the corresponding 10-minute aggregation of the 70 Hz interharmonic components–both with and without the synchronization scheme. It is easy to visualize both the decrease in interharmonic magnitude size and increased correlation with lamp flicker measurement when using the previously described synchronization technique. All following interharmonic measurements were made using this synchronization technique.

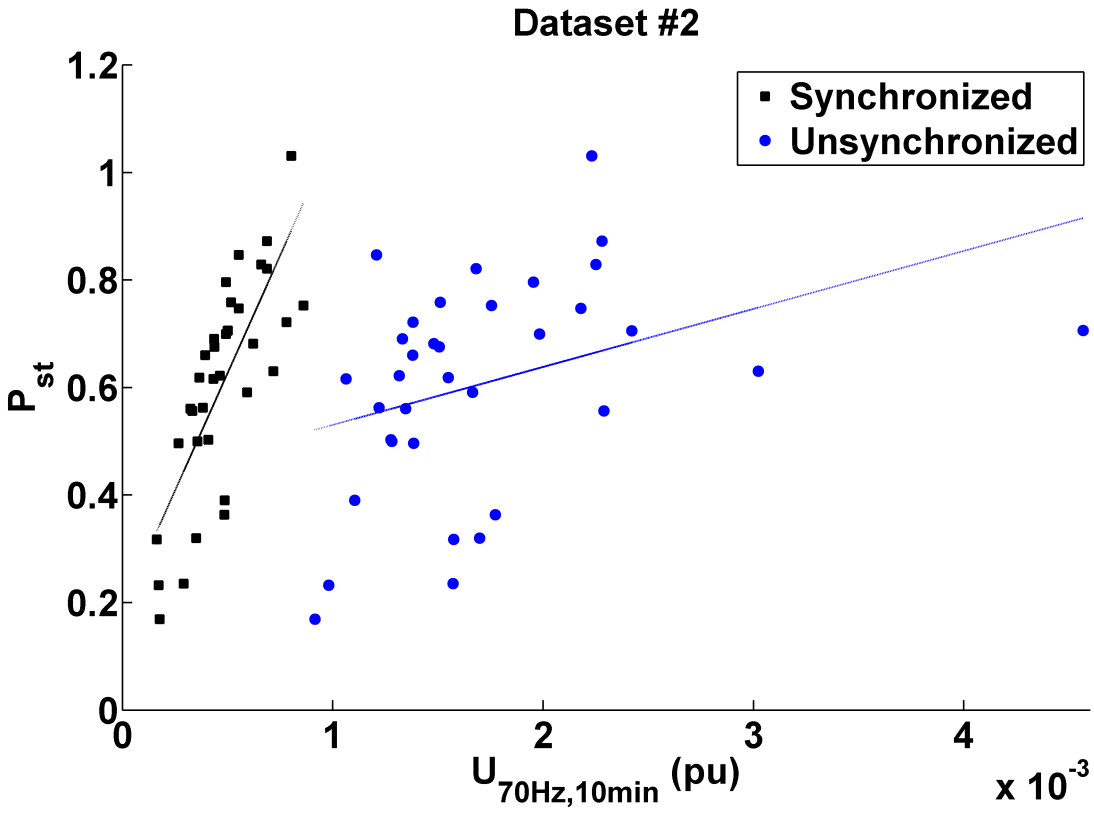

Figure 4.4: Scatter plot of all Dataset 2 P_{st} values versus 10 minute 70 Hz interharmonic values–both with and without the previously described synchronization scheme

An overview of the measurements and calculations made is shown in Figure 4.5. The different type of interharmonic grouping techniques will be described throughout the remainder of this dissertation.

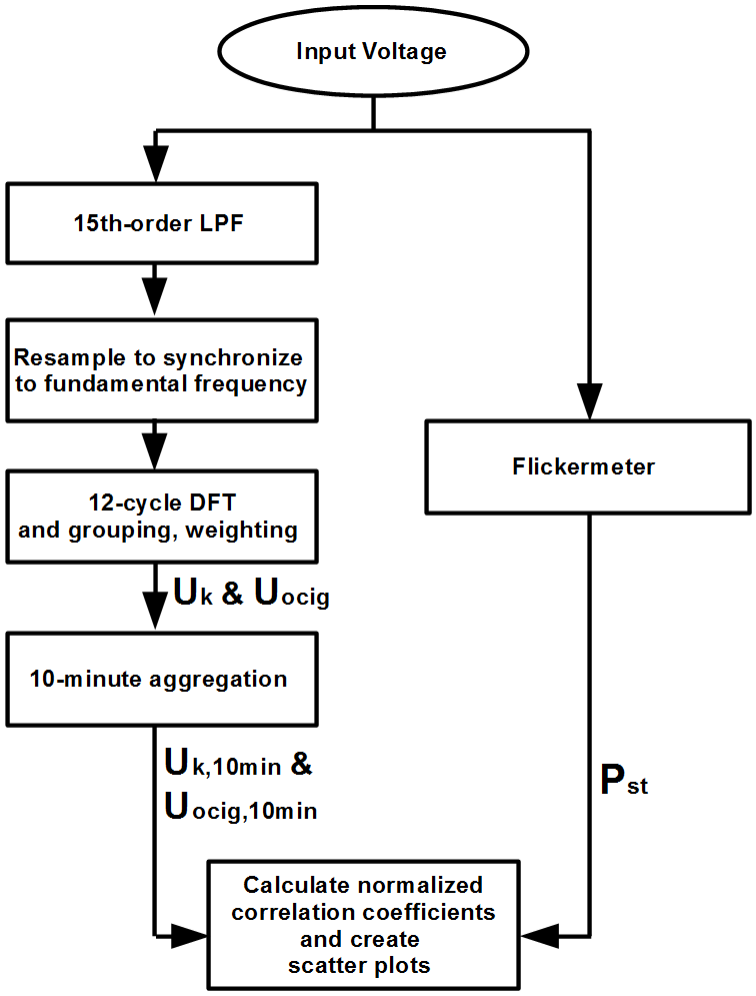

Figure 4.5: Overview of overall process determine level of correlation between measured interharmonics and measured lamp flicker

4.2 Individual Interharmonic Components' Correlations

Firstly, the normalized correlation coefficients for the 10-minute individual interharmonic component measurements through the second harmonic and short-term

flicker severity, U_k *vs.* P_{st}, for all datasets are recorded in Table 4.3. For quicker interpretation, the subscripts of the interharmonic components have been labeled with their frequency value; e.g., R_{11} has been changed to R_{55Hz}.

	Dataset 1	**Dataset 2**	**Dataset 3**	**Dataset 4**	**Dataset 5**	**Dataset 6**
$\mathbf{R}_{5Hz} =$	0.92787	0.61390	0.99040	0.91600	0.63314	0.97787
$\mathbf{R}_{10Hz} =$	0.93438	0.58374	0.99071	0.96092	0.52232	0.96939
$\mathbf{R}_{15Hz} =$	0.93505	0.53588	0.98782	0.96511	0.44169	0.96823
$\mathbf{R}_{20Hz} =$	0.93715	0.52996	0.98928	0.94992	0.060487	0.95909
$\mathbf{R}_{25Hz} =$	0.93866	0.54201	0.98898	0.96778	-0.13386	0.96593
$\mathbf{R}_{30Hz} =$	0.94410	0.56320	0.98853	0.99547	0.23463	0.96818
$\mathbf{R}_{35Hz} =$	0.94856	0.60255	0.99063	0.99326	0.16669	0.97105
$\mathbf{R}_{40Hz} =$	0.95177	0.62144	0.99034	0.99506	-0.02482	0.97068
$\mathbf{R}_{45Hz} =$	0.95977	0.66607	0.98934	0.99394	0.90840	0.97560
$\mathbf{R}_{50Hz} =$	0.96446	0.67876	0.99142	0.99389	0.91166	0.97482
$\mathbf{R}_{55Hz} =$	0.96292	0.70664	0.99061	0.99521	0.91045	0.94190
$\mathbf{R}_{65Hz} =$	0.96851	0.77859	0.99006	0.99728	0.91988	0.95424
$\mathbf{R}_{70Hz} =$	0.96693	0.77078	0.99072	0.99769	0.91056	0.96114
$\mathbf{R}_{75Hz} =$	0.96298	0.71587	0.99107	0.99716	0.90472	0.96204
$\mathbf{R}_{80Hz} =$	0.95677	0.66780	0.99170	0.99690	0.90002	0.96037
$\mathbf{R}_{85Hz} =$	0.95310	0.65711	0.99236	0.99663	0.89540	0.96605
$\mathbf{R}_{90Hz} =$	0.94846	0.63676	0.99235	0.99634	0.88594	0.97279
$\mathbf{R}_{95Hz} =$	0.94510	0.61044	0.99287	0.99598	0.87133	0.96557
$\mathbf{R}_{100Hz} =$	0.94070	0.59670	0.99351	0.99561	0.86680	0.96248
$\mathbf{R}_{105Hz} =$	0.94014	0.63126	0.99372	0.99520	0.87312	0.96603
$\mathbf{R}_{110Hz} =$	0.94569	0.78623	0.99325	0.99476	0.86569	0.96419
$\mathbf{R}_{115Hz} =$	0.94391	0.89190	0.99417	0.99439	0.85958	0.95612

Table 4.3: Normalized correlation coefficients relating individual interharmonic component 10-minute measurements with corresponding P_{st} measurements

As predicted in Section 2.3, short-term flicker severity is the most highly correlated to the interharmonic components distanced 5-10 Hz away from the fundamental,

and the correlation either remains the same or trends downward as the spectral components get further away. For most datasets, most interharmonic components show very strong positive correlation. Although Dataset 5's correlation is not as strong as the others, Dataset 2 exemplifies a clear exception to saying that individual interharmonic component measurements are strongly correlated to measured voltage flicker in general.

4.3 First and Second IEC Interharmonic Groups' Correlation

As previously discussed, the concept of grouping interharmonic components is introduced in [3]. Perhaps better correlation with lamp flicker measurement can be found using a 10-minute aggregation of some kind of interharmonic group rather than individual interharmonic components. It is reasonable to examine the interharmonic groups already defined in the standard before developing a presently unstandardized group. This section documents the correlation coefficients between lamp flicker and the first and second IEC 61000-4-7 interharmonic groups (defined in (2.2.6) and illustrated in Figure 2.5). The same process shown in Figure 4.5 was performed, and the first and second interharmonic groups of (2.2.6) were used as the grouping technique. The resulting correlation coefficients relating each IEC interharmonic group 10-minute aggregation to P_{st} for each dataset are recorded in Table 4.4. The correlation is strong for four of the six datasets, but these results are not improved over considering the individual interharmonic components.

4.4 Magnitude-Only Custom Interharmonic Group Correlation

Because the presently standardized interharmonic groups did not reveal strong correlation in all cases with measured lamp flicker, perhaps an interharmonic group customized to the workings of a standard flickermeter should be examined. This will be accomplished in this section by way of a cursory analysis of a flickermeter.

Dataset #	$\mathbf{U_{ig,0}}$ vs. $\mathbf{P_{st}}$	$\mathbf{U_{ig,1}}$ vs. $\mathbf{P_{st}}$
1	0.95964	0.95902
2	0.67586	0.73802
3	0.97943	0.98246
4	0.99405	0.99611
5	0.74700	0.90759
6	0.96943	0.95492

Table 4.4: Normalized correlation coefficients relating 10-minute aggregations of first and second IEC-defined interharmonic groups measurements (see (2.2.6)) with corresponding P_{st} measurements for all datasets

Consider a general voltage signal as in (4.4.1) that serves as the input to Block 2 of a flickermeter.

$$\begin{aligned} \hat{u}_{B1}(t) = &\cos(\omega_{12}t + \phi_{12}) \\ &+ \sum_{\substack{k=1 \\ k\neq 12}}^{\infty} \hat{U}_k \cos(\omega_k t + \phi_k) \end{aligned} \tag{4.4.1}$$

The indices refer to spectral components with $f_{C,1} = 5$ Hz. Therefore, U_{12}, ω_{12} and ϕ_{12} refer to the magnitude, radian frequency, and phase of the 60 Hz component (the power frequency component); see Figure 2.5 if clarification of this notation is needed. The function in (4.4.1) only represents spectral components with frequencies at multiples of 5 Hz. Theoretically, a signal can have components at any frequency, but the resulting DFT bins will represent spectral components at multiples of 5 Hz if the requirements of [3] are followed. Because of the normalizing effect of Block 1, (4.4.1) is written such that $\hat{U}_k = U_k/U_{12,o}$, where $U_{12,o}$ is the power frequency magnitude averaged using Block 1's low-pass filter.

The squaring demodulator of Block 2 and band-pass filter of Block 3a will have the effect of removing the 60 Hz component and all interharmonic components outside the range of 60 Hz $\pm$ 40 Hz. This restricts the index k of the summation in (4.4.1) to

4 to 20, but, because the band-pass filter is not ideal, it is reasonable to restrict the index to 5 to 19. Therefore, the effects of Block 2 and Block 3a will yield a voltage signal described by (4.4.2). This equation represents the interharmonic components from 25 Hz to 95 Hz.

$$\hat{u}_{B3a}(t) = \sum_{\substack{k=5 \\ k\neq 12}}^{19} \hat{U}_k \cos(\omega_k t + \phi_k) \tag{4.4.2}$$

Block 3b applies a weighting filter based on the $P_{st} = 1.0$ curve. Table A.1 in IEC 61000-3-7 (120 V lamp, 60 Hz system) lists what relative magnitude of rectangular voltage change at a particular frequency will cause a standard flickermeter to measure $P_{st} = 1.0$ if the signal persists for 10 minutes [4]. Because interharmonic components are sinusoidal, it would be better to use magnitudes of sinusoidal voltage changes that cause $P_{st} = 1.0$. Table II in [9] lists such magnitudes. Although [9] is not an internationally accepted standard, the results in that paper formed the basis for the interharmonic limits in IEEE 519-2014 [8]. The sinusoidal magnitudes in Table II of [9] will be used in this dissertation.

These magnitudes are smaller for the frequency components a flickermeter is more sensitive to, so they are inverted to create a weight that will replicate that frequency component's impact on a flickermeter's measurement. An array of weights $W[k]$ is filled from the table with the weight at the k-th index W_k corresponding to the weight for the ω_k frequency. The modulation frequency will correspond to an interharmonic pair equidistant from the power frequency, so interharmonic components equidistant from the power frequency will have the same weight. The weights for the various modulation frequencies are listed in Table 4.5. Notice that the strongest weights are on the 10-Hz amplitude-modulation frequencies. In other words, the interharmonic components at 50 Hz and 70 Hz will be most heavily weighted. This array of weights can be included in the summation in (4.4.2) to obtain the output of Block 3b as

shown in (4.4.3).

W_5, W_{19}	0.25000
W_6, W_{18}	0.35714
W_7, W_{17}	0.47619
W_8, W_{16}	0.71429
W_9, W_{15}	1.14290
W_{10}, W_{14}	2.13220
W_{11}, W_{13}	1.44930

Table 4.5: Weights for specific interharmonic components based on the weighting filter of Block 3b of a standard flickermeter

$$\hat{u}_{B3b}(t) = \sum_{\substack{k=5 \\ k\neq 12}}^{19} W_k \hat{U}_k \cos(\omega_k t + \phi_k) \tag{4.4.3}$$

The concept of interharmonic groups introduced by [3] supports the combining of individual interharmonic components for measurement purposes. For assessing interharmonic measurement and lamp flicker measurement correlation, a custom interharmonic group is established based on the result in (4.4.3). The custom interharmonic group, U_{cig}, is calculated using (4.4.4).

$$\begin{aligned} U_{cig}^2 &= \sum_{\substack{k=5 \\ k\neq 12}}^{19} W_k \hat{U}_k^2 \\ &= \sum_{k=5}^{11} W_k \hat{U}_k^2 + \sum_{k=13}^{19} W_k \hat{U}_k^2 \end{aligned} \tag{4.4.4}$$

The specific interharmonic components included in this custom interharmonic group are also shown in Figure 4.6.

As recommended by [3], the grouping measurement is smoothed as in (2.2.8). The output of this filter will be denoted as U_{ocig}. As required by [10], a 10-minute aggregation is calculated for the custom interharmonic group $U_{cig,10min}$ as in (2.4.1) but using $U_{cig,n}$ instead of $U_{k,n}$. Because these 10-minute aggregations will be made

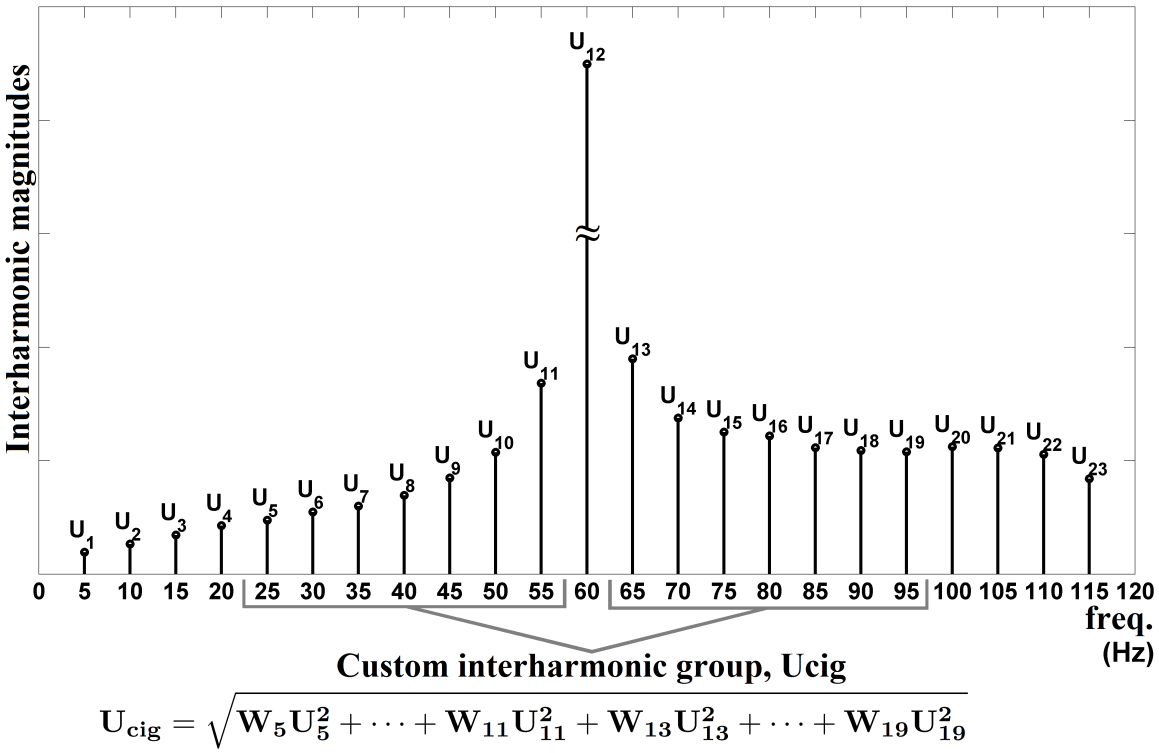

Figure 4.6: Example spectrum showing which interharmonic components are included in the magnitude-only custom interharmonic group for correlation with measured lamp flicker (see (4.4.4))

using the moving average of the weighted, custom interharmonic group (i.e., (2.2.8) applied to (4.4.4)), the measurement to be correlated to measured lamp flicker will be notated as $U_{ocig,10min}$.

The normalized correlation coefficients were calculated for the 10 minute, custom interharmonic group measurements (as shown in (4.4.4)) with respect to the corresponding short-term flicker severity measurement, $U_{ocig,10min}$ *vs.* P_{st}. These values are notated as R_{ocig} and are recorded in Table 4.6.

The normalized correlation coefficients for the magnitude-only custom interharmonic group 10-minute aggregations and P_{st} for each dataset are similar to the results when considering the individual interharmonic component aggregations (compare Table 4.3 to Table 4.6). The correlation for Dataset 5 is somewhat improved when using

Dataset #	$\mathbf{R_{ocig}}$
1	0.96323
2	0.73210
3	0.99016
4	0.99549
5	0.92449
6	0.96542

Table 4.6: Normalized correlation coefficients relating 10-minute aggregations of magnitude-only custom interharmonic group measurements (see (4.4.4)) with corresponding P_{st} measurements for all datasets

the magnitude-only custom interharmonic group rather than the individual interharmonics while the other datasets' correlations remain relatively unchanged.

4.5 Custom Interharmonic Group Based on Scalar Addition of Interharmonic Pairs' Magnitudes

Because components from two IEC interharmonic groups are being considered and because the energy in amplitude modulation is split between interharmonic pairs (as shown in (1.0.1) and (1.0.2)), there is reason to think interharmonic pairs' magnitudes should be added before grouping. A custom interharmonic group was used that added the magnitudes of interharmonic pairs as shown in (4.5.1).

$$\acute{U}^2_{cig} = \sum_{k=1}^{7} W_{12-k}(\hat{U}_{12-k} + \hat{U}_{12+k})^2 \tag{4.5.1}$$

This group effectively performs an arithmetic average on an interharmonic pair's magnitudes before inclusion in the weighted-geometric average. Including the divide-by-2 would simply be including a scaling factor which would not affect a normalized correlation coefficient for linearly related variables.

The process shown in Figure 4.5 was followed using the custom interharmonic group using scalar addition of interharmonic pairs' magnitudes. The correlation results, $\acute{U}_{ocig}$ *vs.* P_{st}, for each dataset are shown in Table 4.7.

Dataset #	$\mathbf{\acute{U}_{ocig}}$ **vs.** $\mathbf{P_{st}}$
1	0.96377
2	0.73742
3	0.98082
4	0.99464
5	0.91621
6	0.96376

Table 4.7: Normalized correlation coefficients relating 10-minute aggregations of custom interharmonic group using scalar addition of interharmonic pairs (as shown in (4.5.1)) with corresponding P_{st} measurements for all datasets

It was found that the grouping method shown in (4.5.1) produced results very similar to (4.4.4). When only magnitudes are being considered, grouping will be performed using (4.4.4) rather than (4.5.1) because it is more consistent with the IEC grouping method shown in (2.2.6) more immediately suggested by the workings of a standard flickermeter.

The calculations for five of the six datasets resulted in strong positive correlation between measured lamp flicker and measured interharmonics when individual interharmonic components or one of the magnitude-only custom interharmonic groups ((4.4.4) or (4.5.1)) is considered. The excepted dataset, Dataset 2, is unique among the loads from which voltage measurements were taken. Though it is not the only arc furnace among the datasets, the load Dataset 2 represents has flicker mitigation equipment installed. It may be that this equipment impacts the ability to correlate lamp flicker measurement with interharmonic measurement. Nonetheless, the results for Dataset 2 do show moderate positive correlation.

Chapter 5

Detailed Analysis of Interharmonics' Impact on Lamp Flicker Measurement

A more detailed examination of an IEC flickermeter is performed to determine if an interharmonic group can be developed that increases the extent of correlation between interharmonic measurement and lamp flicker measurement. What follows is a mathematical and computational analysis of the relationship between interharmonics and voltage flicker. This is accomplished by analyzing the theoretical effects of a flickermeter on a general input voltage containing interharmonics. This investigation is more precise than the cursory one in Section 4.4 used to develop the magnitude-only custom interharmonic group shown in (4.4.4).

Analyzing Blocks 1-3a establishes a theoretical correlation between lamp flicker and particular interharmonic components and informs how interharmonic phasor pairs need to be combined. Block 3b provides a basis for weighting the magnitude results from Block 3a. If an actual estimate of short-term flicker severity was sought, the analysis would need to extend to Block 4 and Block 5. This is unnecessary to simply assess correlation.

This derivation has similarities to the ones provided in [5] and [12]. In an attempt to simplify, the notation here will deviate somewhat from that used in the rest of this dissertation.

5.1 Theoretical Correlation Between Interharmonics and Lamp Flicker

As discussed previously, the flickermeter was developed with respect to amplitude modulation of the fundamental frequency voltage. An expression for a voltage signal

with sinusoidal amplitude modulation is shown again here in (5.1.1) where U_1 and ω_1 are the magnitude and radian frequency of the fundamental component, and U_m and ω_m are the magnitude and radian frequency of the modulation.

$$u(t) = U_1 \sin(\omega_1 t)(1 + U_m \sin(\omega_m t + \phi_m)) \tag{5.1.1}$$

Using the prosthaphaeresis trigonometric identity shown in (5.1.2), the function in (5.1.1) can be rewritten as in (5.1.3).

$$\sin(a)\sin(b) = \frac{1}{2}[\cos(a-b) - \cos(a+b)] \tag{5.1.2}$$

$$u(t) = U_1 \sin(\omega_1 t) + \frac{U_m}{2}\sin((\omega_1 - \omega_m)t - \phi_m) + \frac{U_m}{2}\sin((\omega_1 + \omega_m)t + \phi_m) \tag{5.1.3}$$

It can be seen in (5.1.3) that the amplitude modulation that causes voltage flicker can also be represented as interharmonics.

Consider again the more general voltage signal of (4.4.1) that serves as the input to Block 2 of a flickermeter. This equation is shown again in (5.1.4) for convenience.

$$\begin{aligned} u_{B1}(t) = U_{12}\sin(\omega_{12}t + \phi_{12}) + \sum_{k=1}^{\infty}[&U_{12-k}\sin(\omega_{12-k} + \phi_{12-k}) \\ &+ U_{12+k}\sin(\omega_{12+k} + \phi_{12+k})] \end{aligned} \tag{5.1.4}$$

The indexes refer to spectral components with $f_{C,1} = 5$ Hz. Therefore, U_{12}, ω_{12} and ϕ_{12} refer to the magnitude, radian frequency, and phase of the 60-Hz component. The function in (5.1.4) only represents spectral components with frequencies at multiples of 5 Hz. For brevity, (5.1.4) is rewritten with different notion in (5.1.5).

$$u_{B1}(t) \equiv U_{12}\sin(\omega_{12}t + \phi_{12}) + \sum_{k=1}^{\infty} U_{12\pm k}\sin(\omega_{12\pm k} + \phi_{12\pm k}) \tag{5.1.5}$$

Note that the notation of, for example, $U_{12\pm i}$ is used only for brevity. This analysis, at this point, does not assume that $U_{12-k} = U_{12+k}$ or $\phi_{12-k} = \phi_{12+k}$, although it is true that $\omega_{12} - \omega_{12-k} = \omega_{12+k} - \omega_{12}$. Because Block 1 of the flickermeter normalizes the input voltage, (5.1.5) is rewritten as in (5.1.6).

$$\begin{aligned} \hat{u}_{B1}(t) &= \frac{u_{B1}(t)}{U_{o,12}} \\ &= \sin(\omega_{12}t + \phi_{12}) + \sum_{k=1}^{\infty} \hat{U}_{12\pm k} \sin(\omega_{12\pm k} + \phi_{12\pm k}) \end{aligned} \tag{5.1.6}$$

$\hat{U}_{12\pm k}$ is equal to $U_{12\pm k}/U_{o,12}$. Because the normalizing voltage in Block 1 of the flickermeter is filtered using a first-order low-pass filter with 27.3 sec time constant, the fundamental component used to normalize the interharmonic magnitudes will also be passed through a low-pass filter.

Block 2 squares its input and yields the equation in (5.1.7), given the definitions in (5.1.8).

$$\begin{aligned} u_{B2}(t) &= \hat{u}_{B1}^2(t) \\ &= \frac{1}{2}(1 - \cos 2(\omega_{12}t + \phi_{12})) \\ &+ \sum_{k=1}^{\infty} \hat{U}_{12\pm k}[\cos(\omega_{\pm k}t + \phi_{12} - \phi_{12\pm k}) - \cos(\omega_{24\pm k}t + \phi_{12} + \phi_{12\pm k})] \\ &+ \frac{1}{2}\sum_{k=1}^{\infty} \hat{U}_{12\pm k}^2(1 - \cos 2(\omega_{12\pm k} + \phi_{12\pm k})) \\ &+ \frac{1}{2}\sum_{k=1}^{\infty}\sum_{\substack{j=1 \\ j\neq k}}^{\infty} \hat{U}_{12\pm k}\hat{U}_{12\pm j}[\cos(\omega_{\pm k\pm j}t + \phi_{12\pm k} - \phi_{12\pm j}) \\ &\qquad - \cos(\omega_{24\pm k\pm j}t + \phi_{12\pm k} + \phi_{12\pm j})] \end{aligned} \tag{5.1.7}$$

$$\begin{aligned}
\omega_{\pm k} &= \omega_{12} - \omega_{12\pm k} \\
\omega_{24\pm k} &= \omega_{12} + \omega_{12\pm k} \\
\omega_{\pm k\pm j} &= \omega_{12\pm k} - \omega_{12\pm j} \\
\omega_{24\pm k\pm j} &= \omega_{12\pm k} + \omega_{12\pm j}
\end{aligned} \tag{5.1.8}$$

Because it can be assumed that harmonic and interharmonic components will be orders of magnitude smaller than the fundamental, the cross products (terms with magnitudes of either $U_{12\pm k}^2$ or $U_{12\pm k}U_{12\pm j}$) are considered negligible, and $u_{B2}(t)$ can be simplified as in (5.1.9).

$$\begin{aligned}
u_{B2}(t) \approx{}& \frac{1}{2}(1 - \cos 2(\omega_{12}t + \phi_{12})) \\
&+ \sum_{k=1}^{\infty} \hat{U}_{12\pm k}[\cos(\omega_{\pm k}t + \phi_{12} - \phi_{12\pm k}) - \cos(\omega_{24\pm k}t + \phi_{12} + \phi_{12\pm k})]
\end{aligned} \tag{5.1.9}$$

The band-pass filter in Block 3a has cut-off frequencies of 0.05 Hz and 42 Hz. These respectively eliminate the DC component, $\frac{1}{2}$, the component at $2\omega_{12}$ (because, in this work, $\omega_{12} = 2\pi(60)$) and all components at ω_{24+k}. The components at $\omega_{\pm k}$ and ω_{24-k} avoid attenuation at different values of k. The $\omega_{\pm k}$ components will begin to be severally attenuated once $k > 8$. More careful attention must be given to the ω_{24-k} components. The $24-k$ index causes these components to fall in the pass band from $k = 16$ ($\omega_8 = 2\pi(40)$) to $k = 23$ ($\omega_1 = 2\pi(5)$). Again, this is because if $f_{C,1} = 5$ Hz, then $\omega_{24} = 2\pi(120)$ and $\omega_{16} = 2\pi(80)$; therefore, $\omega_{24} - \omega_{16} = 2\pi(40)$. However, at these values of k, the ω_{24-k} components' magnitudes are non-real values (U_{-4} through U_{-7}). Therefore, the output of Block 3a can be approximated as in (5.1.10).

$$u_{B3a}(t) \approx \sum_{k=1}^{8} \hat{U}_{12\pm k} \cos(\omega_{\pm k}t + \phi_{12} - \phi_{12\pm k}) \tag{5.1.10}$$

Because the band-pass filter is not ideal, it may be appropriate to extend to more or restrict to fewer interharmonic components by adjusting the summation indices.

In this dissertation, the index will be restricted to interharmonics corresponding to $k = 1$ through $k = 7$.

The result in (5.1.10) is a way of looking at voltage signals that cause lamp flicker in terms of interharmonics. Some interpretation of it, particularly in how it relates to amplitude modulation, will be helpful. The index, $12 \pm k$, will range from 5 to 11 and 13 to 19 for $k = 1 : 7$. Because $f_{C,1} = 5$ Hz, these correspond to spectral components from 25 Hz to 55 Hz and 65 Hz to 95 Hz, which can be thought of as the side-bands created by sinusoidal amplitude modulation with frequency ω_k (ranging from 5 Hz to 35 Hz).

The work in [5] points out an interesting phenomena when considering the amplitude modulation which the flickermeter detects. A time-domain sinusoid with frequency ω_x has frequency content at both ω_x and $-\omega_x$. This means the side-bands "to the right" of the -60 Hz component will eventually "wrap around" to positive frequencies. It turns out that sinusoidal amplitude modulation with frequencies ranging from 80 Hz to 160 Hz will also be picked up by the flickermeter (e.g., -60 Hz $-$ (-80) Hz $= 20$ Hz). However, because only one side-band of these modulation frequencies will be detected by the flickermeter, these will have half the impact of sinusoidal modulation of 5 Hz to 40 Hz. The inclusion of these terms in the flickermeter's measurement of lamp flicker is probably a mathematical anomaly because a human eye-brain would not see an incandescent lamp respond to amplitude modulation of these frequencies. However, even if the flickermeter "should not" respond to this kind of amplitude modulation, the aim in this work is explore the correlation between a flickermeter's measurement and interharmonic measurement. The DFT will be equally indiscriminate with what kind of amplitude modulation corresponds to the relevant interharmonics. Therefore, the flickermeter's inclusion of these other sinusoidal amplitude modulation frequencies does not change the result of (5.1.10).

It is essential to see one more relationship between interharmonic pairs and amplitude modulation. The 65 Hz and 55 Hz components with magnitudes and phases of $\hat{U}_{13}$ and $\hat{U}_{11}$, respectively, and ϕ_{13} and ϕ_{11}, respectively, could be thought of as 5 Hz sinusoidal modulation with a magnitude and phase equal to the result of the vector addition $\hat{U}_{13}\underline{/\phi_{13}} + \hat{U}_{11}\underline{/-\phi_{11}}$ (given that $\phi_{12} = 0°$). Under perfect sinusoidal amplitude modulation, $\hat{U}_{13} = \hat{U}_{11}$ and $\phi_{13} = -\phi_{11}$. Real time-varying loads will cause lamp flicker that is not associated with perfect sinusoidal amplitude modulation; however, the magnitude that results from this phasor addition is what is measured by a flickermeter.

That the interharmonic pairs should be combined through phasor addition is inherent in (5.1.10). The component at ω_{+k} and the component at ω_{-k} will add together through phasor addition, but, because their frequencies have opposite signs, the complex conjugate of one will be added to the other. In other words, because $\cos(\alpha) = \cos(-\alpha)$, (5.1.10) can be rewritten as in (5.1.11).

$$\begin{aligned} u_{B3a}(t) \approx \sum_{k=1}^{7} \Big[& \hat{U}_{12-k} \cos(\omega_k t + \phi_{12} - \phi_{12-k}) \\ & + \hat{U}_{12+k} \cos(\omega_k t - (\phi_{12} - \phi_{12+k})) \Big] \end{aligned} \tag{5.1.11}$$

The $\hat{U}_{12-k}$ component and the $\hat{U}_{12+k}$ component will add together through phasor addition as shown in (5.1.12).

$$\begin{aligned} \bar{M}_k &= M_k \underline{/\phi_{M,k}} \\ &= \hat{U}_{12-k}\underline{/\phi_{12} - \phi_{12-k}} + (\hat{U}_{12+k}\underline{/\phi_{12} - \phi_{12+k}})^* \\ &= \hat{U}_{12-k}\underline{/\phi_{12} - \phi_{12-k}} + \hat{U}_{12+k}\underline{/-(\phi_{12} - \phi_{12+k})} \end{aligned} \tag{5.1.12}$$

The magnitude of the phasor resulting from this addition is what impacts lamp flicker measurement. To illustrate the effects of interharmonic pair phasor addition, consider

the functions in (5.1.13) and (5.1.14).

$$y_1(t) = 1\cos(2\pi(60)t + 150^\circ) + 0.003\cos(2\pi(55)t + 93^\circ) + 0.002\cos(2\pi(65)t - 118^\circ) \tag{5.1.13}$$

$$y_2(t) = 1\cos(2\pi(60)t + 150^\circ) + 0.00477806\cos(2\pi(55)t + 70.89^\circ) \tag{5.1.14}$$

If either of these functions describe a voltage signal that persists for 10 minutes, the short-term flicker severity will equal 1.5679. This is because, if the phasor addition shown in (5.1.12) is applied to the interharmonic pair in (5.1.13), the resulting vector is $0.00477806\underline{/70.89^\circ}$. Interestingly, this indicates changing the phase angle of any of the three components in (5.1.13) will affect the P_{st} measurement. However, changing either component's phase in (5.1.14) will not affect the P_{st} measurement.

By combining the interharmonic pairs in (5.1.11) via the phasor addition of (5.1.12), the output of Block 3a can be redefined as in (5.1.15).

$$u_{B3a}(t) \approx \sum_{k=1}^{7} M_k \cos(\omega_k t + \phi_{M,k}) \tag{5.1.15}$$

Block 3b applies the weighting filter described in Section 4.4, and the specific weights were recorded in Table 4.5. The same weights are recorded in Table 5.1 but using subscripts consistent with this section. This array of weights can be included in the summation in (5.1.15) to obtain the output of Block 3b as in (5.1.16).

$$u_{B3b}(t) \approx \sum_{k=1}^{7} W_k M_k \cos(\omega_k t + \phi_{M,k}) \tag{5.1.16}$$

This analysis has shown that there is a theoretical correlation between interharmonics and lamp flicker, suggested which measured interharmonic components will best be correlated to measured lamp flicker, and demonstrated how interharmonic pairs combine and are weighted to influence measured lamp flicker.

W_1	1.44930
W_2	2.13220
W_3	1.14290
W_4	0.71429
W_5	0.47619
W_6	0.35714
W_7	0.25000

Table 5.1: Weights for specific interharmonic components based on the weighting filter of a standard flickermeter

5.2 Grouping and Aggregating Measured Interharmonics for Measured Lamp Flicker Correlation

The concept of interharmonic groups and subgroups introduced by [3] warrants the combining of individual interharmonic components for purposes of measurement. An improved custom interharmonic group is established in this dissertation based on the analysis in Section 5.1. The improved custom interharmonic group, $\tilde{U}_{cig}$, is calculated using the equation in (5.2.1).

$$\tilde{U}_{cig}^2 = \sum_{k=1}^{7} W_k M_k^2 \tag{5.2.1}$$

To help ensure the calculation being made is clear, (5.2.1) can be rewritten in a form showing the calculations made in (5.1.12). This result is shown in (5.2.2). A further illustration of which interharmonic components are being combined and grouped is shown in Figure 5.1.

$$\begin{aligned}\tilde{U}_{cig}^2 = \sum_{k=1}^{7} W_k \Big| & \hat{U}_{12-k} \underline{/\phi_{12} - \phi_{12-k}} \\ & + \hat{U}_{12+k} \underline{/-(\phi_{12} - \phi_{12+k})} \Big|^2\end{aligned} \tag{5.2.2}$$

This grouping measurement is also smoothed as in (2.2.8). The output of this filter will be notated as $\tilde{U}_{ocig}$.

The magnitude-only custom interharmonic group U_{cig} shown in (4.4.4) can be rewritten as in (5.2.3) to replicate the notation developed in the previous section.

$$U_{cig}^2 = \sum_{k=1}^{7} W_k \Big[\hat{U}_{12-k}^2 + \hat{U}_{12+k}^2 \Big] \tag{5.2.3}$$

Because the P_{st} value is calculated over a 10-minute period and each interharmonic measurement, according [3], is made over an approximately 200-millisecond period, approximately 3000 interharmonic measurements are aggregated as required by [10] and discussed in Section 2.4. A 10-minute measurement, $\tilde{U}_{ocig,10min}$, is calculated using the same equation as (2.4.1) but using $\tilde{U}_{ocig,n}$ instead of $U_{k,n}$ (as shown in (5.2.4)).

$$\tilde{U}_{ocig,10min} = \sqrt{\frac{\sum_{n=1}^{3000} \tilde{U}_{ocig,n}^2}{3000}} \tag{5.2.4}$$

The output of the moving average of the n-th improved custom interharmonic group measurement (i.e., (2.2.8) applied to (5.2.2)) is notated as $\tilde{U}_{ocig,n}$. $\tilde{U}_{ocig,10min}$ is the measurement to be correlated to measured lamp flicker.

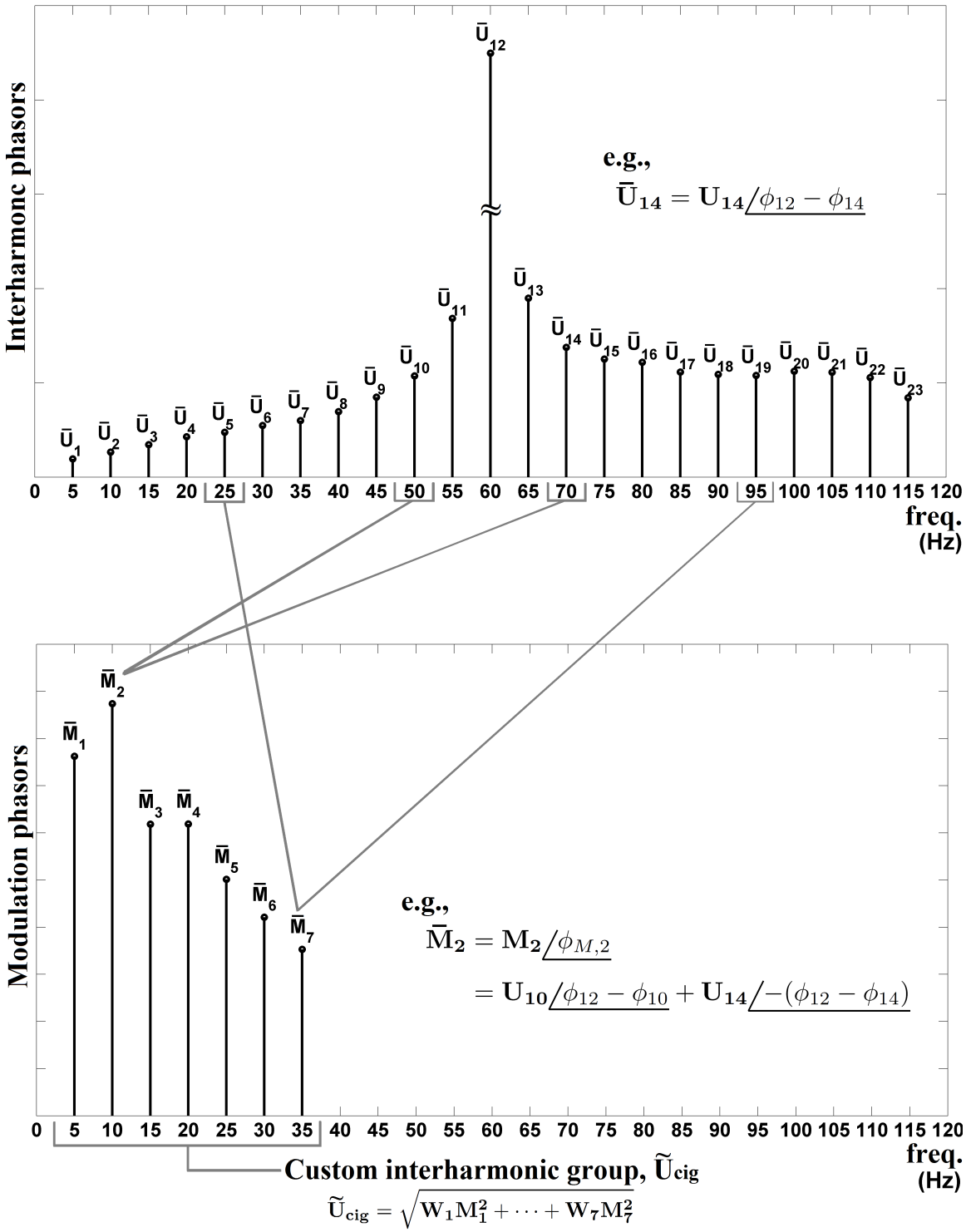

Figure 5.1: Example spectrum showing which interharmonic components are included and how they are combined in the improved custom interharmonic group of (5.2.2) for correlation with measured lamp flicker

Chapter 6

Improved Custom Interharmonic Group Correlation Results

The correlation results of the improved custom interharmonic group is recorded and compared to other results in this chapter. However, another question is first explored: Why might Dataset 2 be the only dataset that requires an interharmonic group utilizing phasor addition of interharmonic pairs to demonstrate strong correlation with measured lamp flicker?

6.1 Analysis of Magnitude-Only Group's Effectiveness

The analysis of the previous subsection concludes that the results of the interharmonic pairs' phasor additions drives what a flickermeter will measure. This prompts the question of why the magnitude-only custom interharmonic group of (5.2.3) gave strong correlation results for five of the six experimental datasets. Only Dataset 2's moderate correlation showed much room for improvement.

First, the relative size of the two individual magnitudes of an interharmonic pair was calculated. The individual interharmonic components' 10-minute aggregations were compared. For example, the relative size of the 5 Hz interharmonic pair (U_{11} and U_{13}) is denoted as $\%U_1$ and is calculated as in (6.1.1).

$$\%U_1 = \frac{|U_{11,10min} - U_{13,10min}|}{U_{11,10min}} \times 100\% \tag{6.1.1}$$

These relative sizes were calculated for the first seven interharmonic pairs (the ones included in the custom interharmonic group) for each dataset for every 10-minute

interval. An arithmetic mean was taken of the 10-minute results. The resulting means are displayed in Table 6.1.

	$\%U_1$	$\%U_2$	$\%U_3$	$\%U_4$	$\%U_5$	$\%U_6$	$\%U_7$
D1:	10%	23%	34%	50%	59%	23%	88%
D2:	11%	28%	48%	79%	84%	87%	120%
D3:	323%	191%	149%	123%	116%	134%	128%
D4:	130%	234%	171%	147%	138%	167%	332%
D5:	83%	82%	90%	260%	191%	205%	548%
D6:	156%	245%	254%	258%	254%	249%	244%

Table 6.1: Arithmetic mean of the relative sizes of interharmonic magnitudes compared to their interharmonic pair for each dataset (D1 through D6); see (6.1.1)

The results in Table 6.1 provide an explanation as to why the phasor addition in the improved group of (5.2.2) was not necessary for Datasets 3 through 6. In each of these sets, one interharmonic component's magnitude is, on average, much larger than its interharmonic pair counterpart. The larger the difference between the magnitudes, the less the phase angle affects the magnitude resulting from phasor addition. For example, $|4\angle 0° + 1\angle 0°| = 5$ while $|4\angle 0° + 1\angle 120°| = 3.61$; a 39% difference. Compare that to $|4\angle 0° + 4\angle 0°| = 8$ while $|4\angle 0° + 4\angle 120°| = 4$; a 100% difference. The large difference in magnitude between the phasor pairs makes including the phase angles far less important for Datasets 3 through 6 as compared to Datasets 1 and 2.

However, Dataset 1 still showed strong correlation between the magnitude-only custom interharmonic group and measured lamp flicker. Therefore the interharmonic pairs' resulting phase angles needed to be analyzed. Adding the magnitudes of interharmonic components while ignoring the phase angles assumes that interharmonic pair's phase angles, relative to the fundamental, are perfect conjugates of one another. In other words, it assumes $\phi_{M,k} = (\phi_{12} - \phi_{12-k}) + (\phi_{12} - \phi_{12+k}) = 0°$; see (5.1.12). The further from 0° these phase angles are, the worse this assumption will be. How well this assumption holds was investigated for Dataset 1 and 2 because, according

to the relative size of interharmonic pairs' magnitudes in these datasets, the phasor relationship of (5.2.2) should be required to show strong correlation between interharmonic and voltage fluctuation measurement. Yet the magnitude-only approach worked well for Dataset 1 while not so well for Dataset 2. This would be explained if the previously mentioned phase-angle assumption was less acceptable for Dataset 2 than Dataset 1.

Because phase angles are not calculated for the 10-minute aggregations, the original 200 ms DFT results were analyzed. The phase angle, $\phi_{M,k}$ was calculated for the seven relevant interharmonic pairs for all 200 ms results. The arithmetic mean of these phase angles were taken over the 10-minute intervals corresponding to the 10-minute custom interharmonic group aggregation intervals. Some statistics on the results are recorded in Table 6.2.

	% of 10-min. intervals with mean $\phi_{M,k} > 80°$	**% of 10-min. intervals with mean $\phi_{M,k} > 100°$**
D1	2.0%	0.0%
D2	48.6%	25.7%

Table 6.2: Statistics about the relationship between interharmonic pairs' phase angles, averaged over 10-minute intervals, for Datasets 1 and 2

These results explain why the magnitude-only approach was not as strong for Dataset 2 as Dataset 1. Approximately 25% of the 10-minute intervals for Dataset 2 had an average phase angle of over 100°, while none did for Dataset 1, indicating the assumption that $\phi_{M,k} = 0°$ is far less accurate for Dataset 2. The 25% of 10-minute intervals with $\phi_{M,k} > 100°$ closely correspond to the top 25% of data points farthest away from Dataset 2's trend line based on the magnitude-only custom interharmonic group (see Figure 6.1).

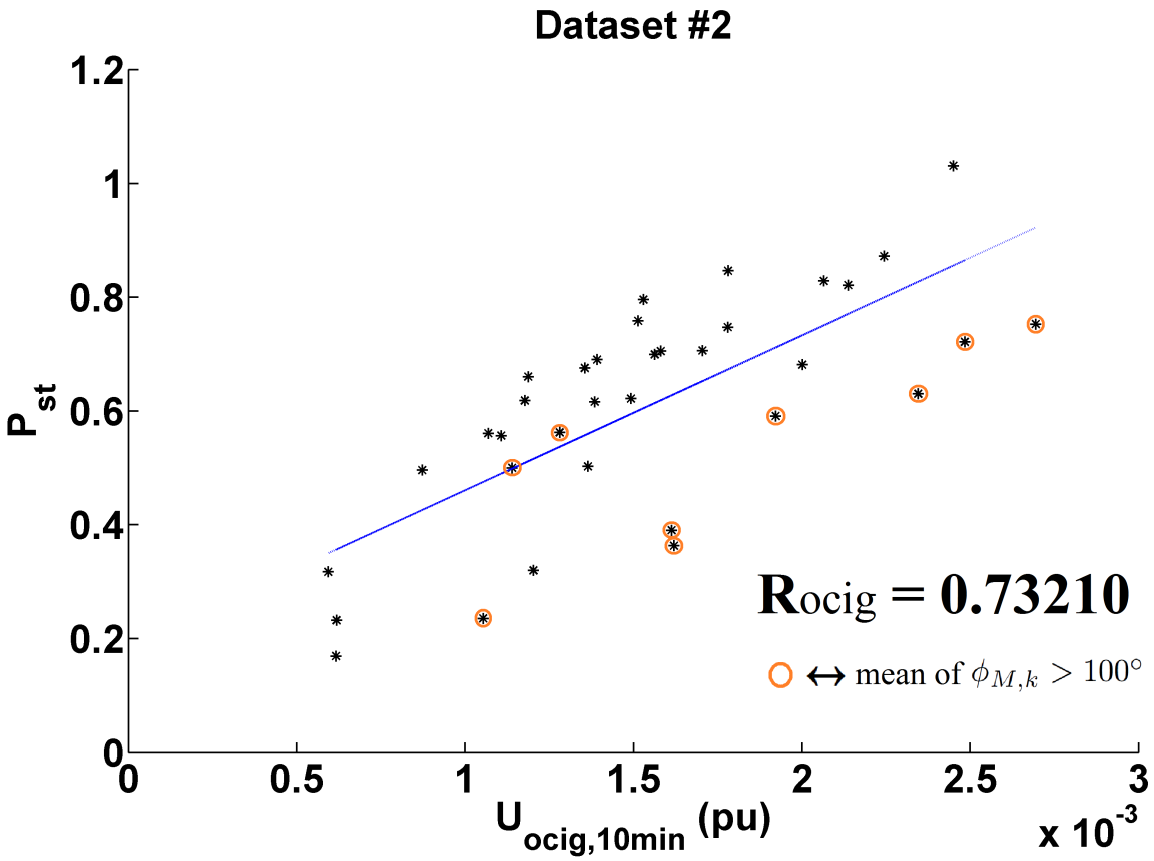

Figure 6.1: Dataset 2: P_{st} measurements versus corresponding 10-minute magnitude-only custom interharmonic group measurements (5.2.3) with data points circled if the mean of all $\phi_{M,k}$ in that 10-minute interval exceed 100°

6.2 Improved Custom Interharmonic Group Correlation

The normalized correlation coefficients for the 10-minute, magnitude-only, custom interharmonic group measurements (as shown in (5.2.3)) versus short-term flicker severity R_{ocig} and the normalized correlation coefficients for the 10-minute, improved custom interharmonic group measurements (as shown in (5.2.2)) versus short-term flicker severity $\tilde{\mathrm{R}}_{ocig}$ are recorded in Table 6.3. The normalized correlation coefficients for the magnitude-only-based custom interharmonic groups and P_{st} for each dataset are comparable to the results when considering the individual interharmonic component aggregations (compare Table 4.3 to Column 2 of Table 6.3). The magnitude-only

Dataset #	$\mathbf{R_{ocig}}$	$\mathbf{\tilde{R}_{ocig}}$
1	0.96324	0.96528
2	0.73270	0.95102
3	0.99012	0.98962
4	0.99561	0.99705
5	0.92491	0.95124
6	0.96478	0.95830

Table 6.3: Normalized correlation coefficients relating 10-minute aggregations of custom interharmonic groups measurements (see (5.2.3) for R_{ocig} and (5.2.2) for $\tilde{R}_{ocig}$) with corresponding P_{st} measurements for all datasets

custom interharmonic group measurement based on (5.2.3) does not improve the generality of the claim that interharmonic measurement are strongly correlated with lamp flicker measurement.

Using the improved custom grouping method based on (5.2.2), the normalized correlation coefficients for Dataset 2 and Dataset 5 are over 95%. These results are significant because strong correlation between interharmonic measurement and lamp flicker measurement is shown to exist for all six datasets. The grouping method based on (5.2.3) gave very similar results to the results of considering only the individual interharmonic components. Only when the interaction of the interharmonic pairs is considered does the correlation between interharmonics and lamp flicker potentially significantly increase over against consideration of the individual interharmonic component magnitudes.

Scatter plots of lamp flicker measurement versus interharmonic measurement were created for Dataset 1 for both interharmonic grouping techniques; see Figures 6.2 and 6.3. Dataset 1 results are shown because it contains the most data and because it exemplifies the five datasets for which correlation strength is about the same regardless of interharmonic grouping technique. Scatter plots were also generated for

Dataset 2 to help visualize the improvement of grouping interharmonics using (5.2.2) as opposed to (5.2.3); see Figures 6.4 and 6.5.

Five of six datasets record strong positive correlation between measured lamp flicker and measured interharmonics when individual interharmonic components or a magnitude-only custom interharmonic group based on (5.2.3) is considered. Only when the interharmonic components are grouped according to (5.2.2) is strong correlation calculated for all six datasets.

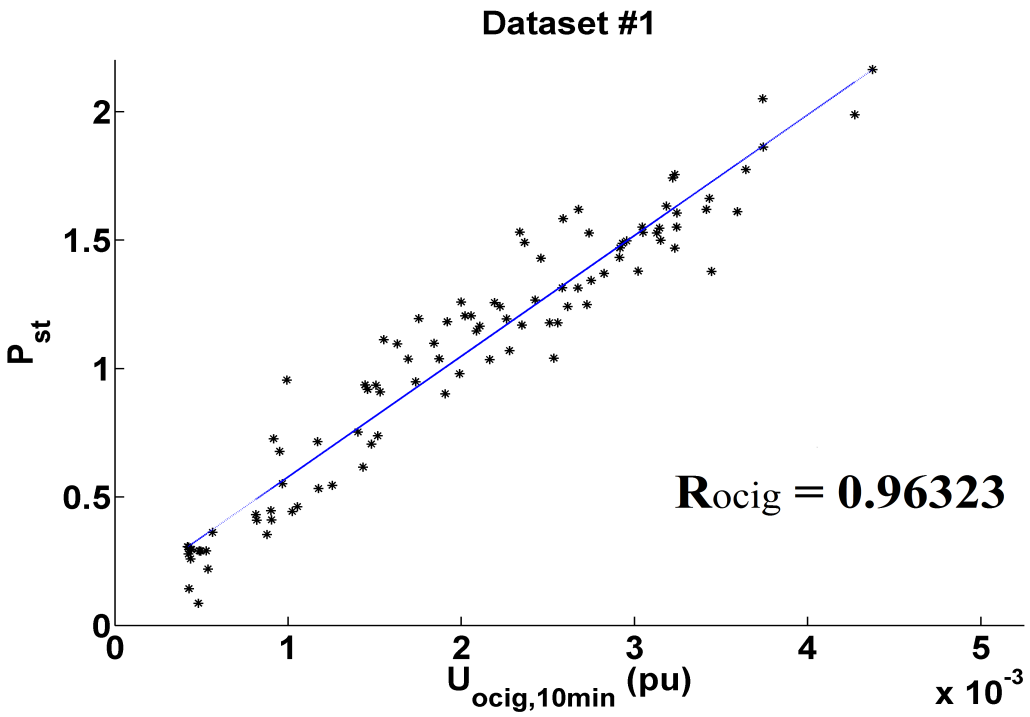

Figure 6.2: Dataset 1: P_{st} measurements versus corresponding 10-minute magnitude-only custom interharmonic group measurements (5.2.3)

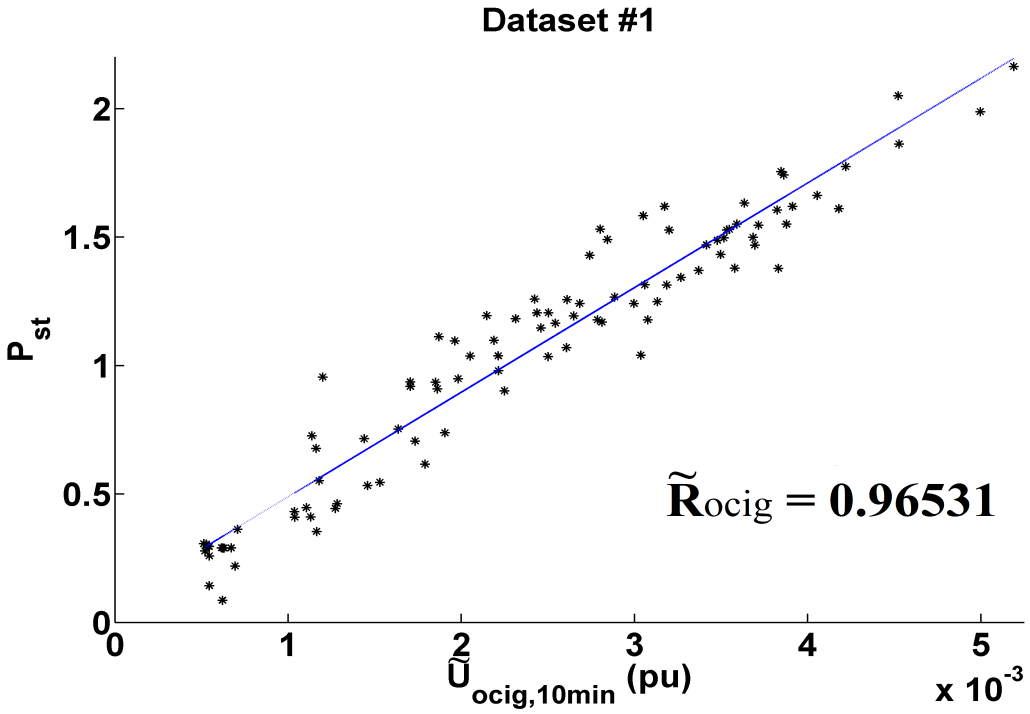

Figure 6.3: Dataset 1: P_{st} measurements versus corresponding 10-minute improved custom interharmonic group measurements (5.2.2)

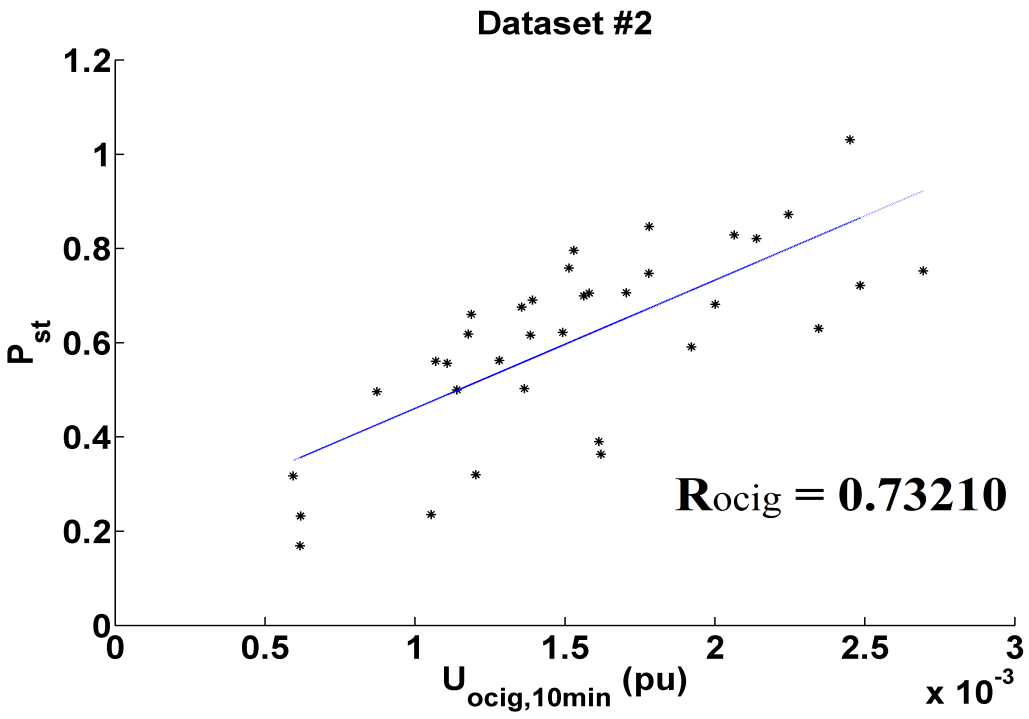

Figure 6.4: Dataset 2: P_{st} measurements versus corresponding 10-minute magnitude-only custom interharmonic group measurements (5.2.3)

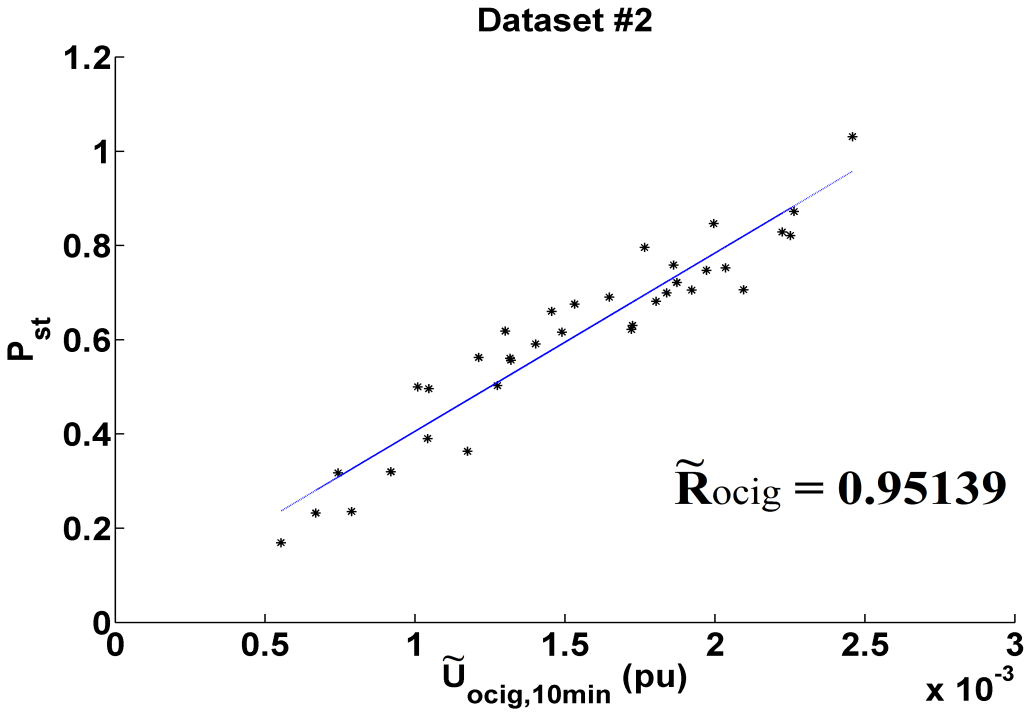

Figure 6.5: Dataset 2: P_{st} measurements versus corresponding 10-minute improved custom interharmonic group measurements (5.2.2)

Chapter 7

Conclusion

In this dissertation, the general correlation between measured interharmonics and measured voltage fluctuations, specifically lamp flicker, has been assessed. There exists a need to quantify and measure voltage fluctuations more broadly than lamp flicker. Measuring interharmonics has been suggested as a means of characterizing voltage fluctuations due to the present existence of an international standard for measuring them and their theoretical equivalence to amplitude modulation, the present focus of standard flickermeters. However, any proposed method for future measurement of voltage fluctuations must first be demonstrated to provide results consistent with presently standardized methods. Therefore, the first step for assessing the general suitability of measuring interharmonics as the basis of voltage fluctuation quantification and eventual emission limitation is establishing a general correlation between measured interharmonics and measured lamp flicker.

Whether or not a general correlation exists was investigated using voltage measurements taken at six different industrial facilities. Each dataset contains multiple hours of measurements. Various interharmonic measurements were aggregated over 10 minutes and compared to the corresponding 10 minute short-term flicker severity measurements. This comparison was quantified by calculating the normalized correlation coefficient between the interharmonic and lamp flicker measurements for each dataset. All measurements and calculations were performed in compliance with IEC 61000-4-7, 61000-4-15 and 61000-4-30.

Strong positive correlation was found for five of the six datasets when only interharmonic magnitudes were considered—whether individual interharmonic components or a custom interharmonic group based on the workings of a standard flickermeter were considered. In one case only moderate positive correlation was found. This dataset corresponds to an industrial load with flicker mitigation equipment installed. This may be the reason the grouping approach based solely on interharmonic magnitudes revealed strong correlation for all datasets apart from this one.

A more detailed analysis of a standard flickermeter was performed and an improved custom interharmonic group for correlating to measured voltage fluctuation was developed. By combining interharmonic pairs through phasor addition and grouping the resulting magnitudes, strong positive correlation was recorded for all six datasets. It is concluded from these results that measured interharmonics and measured lamp flicker are strongly correlated in general. It is noteworthy that by far the most critical aspects of the interharmonic measurements for demonstrating correlation with lamp flicker measurement are the synchronization of the voltage samples with the power frequency and the phasor addition of the interharmonic pairs.

The first critical task to justify basing general voltage fluctuation measurements on interharmonic measurements has been accomplished in this dissertation. Furthermore, it is suggested by the results that measuring interharmonics might offer advantages over the present approach for measuring voltage fluctuations. The analysis in this dissertation showed how the flickermeter responds to interharmonics. The results of the analysis were confirmed through experimentation. This same process could be repeated to determine ways of characterizing voltage fluctuations' impact on other luminous lamps and power system equipment. After introducing a means of characterization, such as through other custom interharmonic groups with other weights, harmful levels of voltage fluctuation could be established for various devices, guiding the development of emission limits. Research undertakings such as these

constitute the next necessary steps if voltage fluctuation quantification, measurement and compliance are to be transitioned to interharmonic measurement.

Bibliography

[1] IEC 61000-4-15 Ed. 2: Electromagnetic compatibility (EMC) – Part 4-15: "Testing and measurement techniques – Flickermeter – Functional and design specifications."

[2] Gallo, D.; Landi, C.; Langella, Roberto; Testa, Alfredo, "On the Use of the Flickermeter to Limit Low-Frequency Interharmonic Voltages," Power Delivery, IEEE Transactions on, vol.23, no.4, pp.1720,1727, Oct. 2008.

[3] IEC 61000 4-7, Electromagnetic compatibility (EMC) – Part 4-7: "Testing and measurement techniques âĂŞ General guide on harmonics and interharmonics measurements and instrumentation, for power supply systems and equipment connected thereto."

[4] "Electromagnetic compatibility (EMC) – Part 3-7: Limits – Assessment of emission limits for the connection of fluctuating installations to MV, HV and EHV power systemsâĂŤBasic EMC Publication IEC Tech. Rep. 61000-3-7, 2008, Ed. 2.0.

[5] Gallo, D.; Langella, Roberto; Testa, Alfredo, "Light flicker prediction based on voltage spectral analysis," Power Tech Proceedings, 2001 IEEE Porto, vol.1, pp.6, 2001.

[6] Gallo, D.; Langella, R.; Testa, A., "Toward a new flickermeter based on voltage spectral analysis," Industrial Electronics, 2002. ISIE 2002. Proceedings of the 2002 IEEE International Symposium on, vol.2, pp.573,578 vol.2, 2002.

[7] Tayjasanant, T.; Wencong Wang; Chun Li; Wilsun Xu, "Interharmonic-flicker curves," Power Delivery, IEEE Transactions on, vol.20, no.2, pp.1017,1024, April 2005.

[8] IEEE Std. 519-1992 Recommended Practices and Requirements for Harmonic Control in Electric Power Systems.

[9] Halpin, S.M.; Singhvi, V., "Limits for Interharmonics in the 1-100-Hz Range Based on Lamp Flicker Considerations," Power Delivery, IEEE Transactions on, vol.22, no.1, pp.270,276, Jan. 2007.

[10] IEC 61000 4-30, Electromagnetic compatibility (EMC) – Part 4-30: "Testing and measurement techniques – Power quality measurement methods."

[11] Barros, J.; Prez, E.; Pigazo, A.; Diego, R.I., "Simultaneous measurement of harmonics, interharmonics and flicker in a power system for power quality analysis," Power System Management and Control, 2002. Fifth International Conference on (Conf. Publ. No. 488), pp.100,105, 17-19 April 2002.

[12] Hernandez, A.; Mayordomo, J.G.; Asensi, R.; Beites, L.F., "A new frequency domain approach for flicker evaluation of arc furnaces," Power Delivery, IEEE Transactions on, vol.18, no.2, pp.631,638, April 2003.

[13] Kose, N.; Salor, O., "A new frequency domain approach for light flicker evaluation of power systems," Instrumentation and Measurement Technology Conference, 2009. I2MTC '09. IEEE , pp.618,623, 5-7 May 2009.

[14] Gunther, E.W., "Interharmonics in power systems," Power Engineering Society Summer Meeting, 2001, vol.2, pp.813,817 vol.2, 2001.

[15] Cigre/CIRED CC02 Voltage Quality Working Group and IEEE Interharmonic Task Force, "Interharmonics in Power Systems," 1 Decemeber 1997.

[16] IEEE Task Force on Harmonics modeling and Simulation "Interharmonics: Theory and Modeling," IEEE Transactions on Power Delivery, Vol. 22, No. 4, October 2007, p. 2335-2348.

[17] Gallo, D.; Langella, R.; Testa, A., "On the processing of harmonics and interharmonics in electrical power systems," Power Engineering Society Winter Meeting, 2000. IEEE, vol.3, pp.1581,1586 vol.3, 23-27 Jan 2000

[18] Testa, A.; Gallo, D.; Langella, R., "Interharmonic measurements in IEC standard framework," Power Engineering Society Summer Meeting, 2002 IEEE, vol.2, no., pp.935,940 vol.2, 25-25 July 2002.

[19] Feola, L.; Langella, R.; Testa, A., "On the Effects of Unbalances, Harmonics and Interharmonics on PLL Systems," Instrumentation and Measurement, IEEE Transactions on, vol.62, no.9, pp.2399,2409, Sept. 2013.

[20] Taekhyun Kim; Powers, E.J.; Grady, W.M.; Arapostathis, A., "Detection of Flicker Caused by Interharmonics," Instrumentation and Measurement, IEEE Transactions on, vol.58, no.1, pp.152,160, Jan. 2009.

[21] Drapela, J.; Toman, P., "Interharmonic - Flicker Curves of Lamps and Compatibility Lever for Interharmonic Voltages," Power Tech, 2007 IEEE Lausanne, pp.1552,1557, 1-5 July 2007.

[22] Cheng-I Chen; Chang, G.W., "An accurate time-domain procedure for harmonics and interharmonics detection," Power and Energy Society General Meeting, 2010 IEEE, pp.1,1, 25-29 July 2010.

[23] Valenzuela, J.; Pontt, J., "Real-time interharmonics detection and measurement based on FFT algorithm," Applied Electronics, 2009. AE 2009, pp.259,264, 9-10 Sept. 2009.

[24] Hsiung Cheng Lin, "Power Harmonics and Interharmonics Measurement Using Recursive Group-Harmonic Power Minimizing Algorithm," Industrial Electronics, IEEE Transactions on, vol.59, no.2, pp.1184,1193, Feb. 2012.

[25] Feifei Li; Maoqing Ye, "Calculation of Flicker Parameters Using Voltage Interharmonics," Power and Energy Engineering Conference (APPEEC), 2012 Asia-Pacific, pp.1,4, 27-29 March 2012.

[26] Gallo, D.; Langella, Roberto; Testa, Alfredo, "Desynchronized Processing technique for Harmonic and interharmonic analysis," Power Delivery, IEEE Transactions on, vol.19, no.3, pp.993,1001, July 2004.

[27] D. Gallo, R. Langella, and A. Testa, "A self tuning harmonics and interharmonics processing technique," Eur. Trans. Elect. Power, vol. 12, no. 1, pp. 25-31, Jan./Feb. 2002.

[28] George R. Cooper and Clare D. McGillem, "Elements of Statistics" in *Probabilistic Methods of Signal and System Analysis*, 3rd ed. New York, Oxford University Press, 1999.

Appendix A

Alternative Improved Custom Interharmonic Groups

Correlation between lamp flicker and interharmonic measurements was assessed under other conditions. The following documents the differences in setup and/or interharmonic group and the resulting correlation coefficients.

To explore the significance of the interharmonic weights, the improved custom interharmonic group of (5.2.2) was implemented without the weight factor W_k as shown in (A.0.1).

$$\tilde{U}^2_{cig,noW_k} = \sum_{k=1}^{7} \Big| \hat{U}_{12-k} \underline{/\phi_{12} - \phi_{12-k}} + \hat{U}_{12+k} \underline{/-(\phi_{12} - \phi_{12+k})} \Big|^2 \tag{A.0.1}$$

The process shown in Figure 4.5 was followed using the improved custom interharmonic group with no weights. The correlation results for each dataset are shown in Column 2 of Table A.1. These results are almost identical to those of the custom interharmonic group with the weighting factor. Dataset 5 is possibly excepted with about 5% lower correlation.

The importance of the exact number of terms to include in the improved custom interharmonic group was also explored. The normalized correlation coefficients were calculated again using the group shown in (5.2.2) but only three interharmonic pairs were included, as shown in (A.0.2), instead of seven. The results are recorded in

Column 3 of Table A.1.

$$\tilde{U}^2_{cig,3Pairs} = \sum_{k=1}^{3} W_k \Big| \hat{U}_{12-k} \underline{/\phi_{12} - \phi_{12-k}} + \hat{U}_{12+k} \underline{/-(\phi_{12} - \phi_{12+k})} \Big|^2 \tag{A.0.2}$$

The correlation results are only slightly weaker than the results of the improved group which includes seven pairs (5.2.2). The comparisons made in this chapter show that, for correlating interharmonics at these six datasets to lamp flicker, combining interharmonic pairs' effects through phasor addition is far more important than the precise number of interharmonic components or weighting factors included in the grouping method.

Dataset	**P_{st} versus**		
#	$\tilde{\mathbf{U}}_{\mathbf{ocig}}$	$\tilde{\mathbf{U}}_{\mathbf{ocig,noW_k}}$	$\tilde{\mathbf{U}}_{\mathbf{ocig,3Pairs}}$
1	0.96528	0.96420	0.96544
2	0.95102	0.94760	0.95148
3	0.98962	0.97929	0.98960
4	0.99705	0.99680	0.99687
5	0.95124	0.90327	0.93682
6	0.95830	0.96385	0.95573

Table A.1: Normalized correlation coefficients for all datasets relating P_{st} measurements with corresponding 10-minute aggregations of improved custom interharmonic group using seven pairs and original weights (as shown in (5.2.2)), using seven pairs and no weights (as shown in (A.0.1)) and using three pairs and original weights (as shown in (A.0.2))

Appendix B

Correlation Results With and Without the Two Low-pass Filters

The overall process used in this dissertation for calculating the improved custom interharmonic group utilized two fifteenth-order, low-pass Butterworth filters. The first filter was used before the synchronizing scheme and DFT to remove frequencies above 150 Hz—those not of interest in this dissertation. The second was employed at the end of the synchronization scheme before the DFT because of the spectral content generated through linear interpolation (a linear interpolator's frequency response is a sinc^2 function). The impact of removing these low-pass filters on the correlation results was explored. These low-pass filters are the most computationally-intensive aspects of the entire process. If the process for calculating group interharmonic values were to be implemented in real-time, whether or not these low-pass filters can be removed or much lower-order filters used in their place is significant.

The resulting correlation coefficients were calculated with neither filter used in the process. The process shown in Figure 4.5 was repeated but without the first low-pass filter block. Also, the synchronization block, the details of which are shown in 4.3, is implemented without the low-pass filter at the end. The results are shown in Column 2 of Table B.1. For five of the datasets, the correlations are largely unchanged. Only Dataset 3's results were weaker when the two low-pass filters were removed (0.98962 compared to 0.83746).

To test if only one of the filters was important for Dataset 3, the experiment was repeated with only the second low-pass filter removed. The low-pass filter before the DFT was included. The results are shown in Column 3 of Table B.1. Dataset 3's results returned to the values present before both filters were removed (0.98962

versus 0.98898). The results with only the first low-pass filter included are just as strong as the results with both filters included. It appears that only the first low-pass filter has any potential impact on the strength of correlation results.

Whether or not a lower-order filter could be used in place of the front-end fifteenth-order, low-pass butterworth filter was explored. The front-end filter was replaced with a first-order, low-pass butterworth filter with the same cut-off frequency, 150 Hz. The results are shown in Column 4 of Table B.1. Interestingly, the results using a first-order low-pass filter for the first filter and not using the second filter at all are at least as strong as the results using both fifteenth-order filters. This suggests the second filter is not necessary, and it is not necessary to use a high-order filter before the synchronization scheme and DFT calculation.

Dataset #	$\tilde{\mathbf{R}}_{\mathbf{ocig}}$ **for processes using different filters**			
	Both filters	**Neither filter**	**1st filter only**	**1st filter changed to 1st-order**
1	0.96528	0.96512	0.96547	0.96497
2	0.95102	0.95065	0.95176	0.95158
3	0.98962	0.83746	0.98898	0.98920
4	0.99705	0.99789	0.99784	0.99788
5	0.95124	0.96297	0.96831	0.97584
6	0.95830	0.97140	0.97234	0.97056

Table B.1: Normalized correlation coefficients relating 10-minute aggregations of weighted improved custom interharmonic group with corresponding P_{st} measurements for all datasets, though the process was run with different combinations of filters present

Appendix C

Estimating Short-Term Flicker Severity Using Interharmonic Measurements

By introducing a scaling factor K on the improved interharmonic group's 10-minute values, a loose estimate for short-term flicker severity can be calculated. By picking a point that falls on the scatter plot's trend-line, a scaling factor can be calculated that scales the interharmonic group value to the P_{st} value. This was only performed on Dataset 1 and Dataset 2 because the other datasets' measurement multipliers and bases are not exactly known so the scaling factor for them would have to be calculated for each individual dataset.

A scaling factor of 429 was added to the custom interharmonic group of (5.2.2) to calculate an estimated short-term flicker severity value $P_{st,est}$ as shown in (C.0.1).

$$P_{st,est} = K\Bigg(\sum_{k=1}^{7} W_k \Big|\hat{U}_{12-k}\underline{/\phi_{12}-\phi_{12-k}} + \hat{U}_{12+k}\underline{/-(\phi_{12}-\phi_{12+k})}\Big|^2\Bigg)^{1/2} \tag{C.0.1}$$

These values were calculated for all 10-minute intervals of Dataset 1 and Dataset 2. For brevity, only the estimated short-term flicker severity values for Dataset 2 are recorded in Table C.1 along with the corresponding measured short-term flicker severity and the percent difference between the estimate and the measurement.

The arithmetic mean of all the percent differences between all Dataset 1 and Dataset 2 estimated and measured short-term flicker severity values is 13.2%. A better estimate for P_{st} is probably attainable by implementing the transfer function, binning process, and statistical calculation of Blocks 4 and 5 of the flickermeter.

Estimated $P_{st,est}$	**Measured P_{st}**	**% Difference**
0.972	0.872	10.3%
0.338	0.235	30.5%
0.433	0.500	-15.4%
0.739	0.622	15.9%
0.287	0.232	19.2%
0.640	0.616	3.7%
0.707	0.690	2.4%
0.790	0.699	11.4%
0.741	0.630	14.9%
0.857	0.847	1.2%
0.237	0.169	28.7%
0.804	0.722	10.3%
0.547	0.503	8.2%
0.449	0.496	-10.5%
0.967	0.821	15.1%
0.602	0.591	1.8%
0.846	0.747	11.7%
0.900	0.706	21.5%
0.758	0.796	-5.0%
0.395	0.320	19.0%
0.826	0.705	14.6%
0.505	0.363	28.0%
0.566	0.557	1.7%
0.800	0.759	5.1%
0.447	0.390	12.7%
0.521	0.562	-8.0%
1.056	1.031	2.3%
0.774	0.681	12.0%
0.658	0.676	-2.7%
0.558	0.618	-10.7%
0.625	0.660	-5.7%
0.565	0.561	0.8%
0.319	0.317	0.6%
0.955	0.829	13.2%
0.874	0.753	13.9%

Table C.1: Short-term flicker severity estimates based on (C.0.1) compared to the measured values